FLUORINATED STYRENE POLYMERS FOR OPTICAL WAVEGUIDES

Elizabeth Sara Maron

Department of Chemistry, McGill University, Montreal August 2008

A thesis submitted to McGill University in partial fulfillment of the requirements of the degree of Master of Science

© Elizabeth Sara Maron, 2008

ABSTRACT

A series of fluorinated copolymers were prepared and used to fabricate optical waveguides by photolithography. Reproducible syntheses were established for a buffer material, 4 — fluoro-styrene-co-pentafluoro-styrene-co-[4-styren-4'-yl-2,3,5,6-tetrafluorophenylether] (bufTxx), a nd gui ding m aterial, S tyrene-co-penta-fluorostyrene-co-[4-styren-4'-yl-2,3,5,6-tetrafluorophenyl-ether] (terTxx), as well as their precu rsors. The p olymers were cha racterized by attenuated total r eflection Fourrier t ransform i nfrared spectroscopy (A TR F T-IR), gel pe rmeation chromatography (GPC), proton nuclear magnetic resonance spectroscopy (¹H NMR), and thermal ana lyses. Freestanding waveguide st ructures and multilayer bu ried waveguide devices were prepared on silicon substrates. The guiding polymer behaved as a negative resist, facilitating photoinitiated lithographic printing. These structures were i nvestigated by optical m icroscopy, f ield-emission gun scanning e lectron microscopy (FEG S EM) and prism coupling an alysis. A 63 2 nm H eNe l aser w as successfully end-coupled to printed waveguide structures from an optical fiber.

RÉSUMÉ

Une série de copolymères fluorés a été préparée et employée pour fabriquer des guides d'ondes optiques par photolithographie. Des synthèses reproductibles ont été établies po ur un m atériel tampon, l e 4 -fluorostyrène-co-pentafluorostyrène--co-[4-(styrèn-4'-yl)-2,3,5,6-tétrafluorophényléther] (bufTxx), pour le matériel de guidage, d u s tyrène-co-pentafluorostyrène-co-4-(styrèn-4'-yl)-2,3,5,6-tétra-fluoro--phényléther] (terTxx), ainsi que leurs précurseurs. Les polymères ont été caractérisés par spectroscopie infrarouge par transformé de Fourier de type réflexion totale atténué (ATR FT-IR), par c'hromatographie s'ur gel perméable (GPC), par s'pectroscopie de résonance magnétique nuc léaire de proton (¹H R MN), ainsi que par de s an alyses thermiques. Des motifs de gui des d'ondes i ndépendants et de s di spositifs de gui de d'ondes à plusieurs couches ont été préparés sur des substrats de silicium. Le polymère agissant comme guide d'ondes a des propriétés de résistances négatives, facilitant une impression l'ithographique phot oinitiée. C es motifs ont été étudiés par microscopie optique, par microscopie é lectronique de ba layage utilisant un c anon à émission de champ (FEG SEM) et par analyse de couplage par prisme. Un laser de 632 nanomètres (HeNe) a ét é couplé avec suc cès aux motifs de guide d'ondes imprimées d'une fibre optique.

ACKNOWLEDGEMENTS

I give my sincere thanks to the following individuals:

My supervisor, Professor Mark P. Andrews, for his guidance, especially in the final hectic weeks.

Petr Fiurasek of CSACS for his help with IR, DSC, and TGA data collection, and for his graceful handling of my inability to write down instructions. Vito Logiudice of MIAM for his patience with my emails and cleanroom's cheduling habits. Mattieu Nanini for microfab training and assistance with the ever-stubborn a ligner. Tony Azzam for finding the time to run my many GPC samples and Line Mongeon for her 11th hour assistance with FEG SEM.

All of the members of the Andrews group during my tenure there, especially the following: Nicolas Belanger for imparting his laboratory wisdom, particularly on the benefits of routine and attentiveness and the horrors of dust. Nicolas Duxin for acting as my extra pair of hands and providing hours of entertainment during long cleanroom hours. Marie-Pascale Manseau for sharing her preliminary work and learning about NaH the hard way so that I wouldn't have to. Francis Loiseau for translating my abstract and counting in Roman numerals to kill the monotony of the undergraduate lab. Jennifer Lofgreen for lending me her ear and her shoulder and for sharing my appreciation of fine kitchen equipment.

Eva Dias for helping me to maintain my sanity during a string of successive IPs and for accepting the role of thesis submission savior.

Patrick Farber, who was always available for spontaneous and necessary work breaks and who is keeping New York sarcasm alive in Canada.

Jill B isgard, the superintendent of 495 P rince A rthur, for being a constant encouraging voice over five years, three apartments, and three roommates.

Chantal Marotte for her administrative assistance as well as our in-person and long distance conversations, which revived my spirit on many occasions.

And finally, Timothy Andrew Cernak, who has now repaid my support during his thesis writing by supporting me through mine, twice.

TABLE OF CONTENTS

Title Page	i
Abstract	ii
Résumé	iii
Acknowledgements	iv
Table of Contents	v
CHAPTER 1 Introduction and Background	1
1.1 O ptical Waveguides	1
1.1.1 Theoretical Description of Waveguiding	3
1.1.2 O ptical Loss	8
1.1.3 Processing and Fabrication	9
1.2 P olymers in Optics	11
1.2.1 Characteristics for Optical Applications	11
1.2.2 Vibrational Loss in Polymers	12
1.2.3 Review of Polymers for Optical Waveguides	14
1.2.3.1 P olysiloxanes	15
1.2.3.2 P olyacrylates	16
1.2.3.3 P olyimides	17
1.2.3.4 Fluorinated Arene Polymers	18
CHAPTER 2 Preparation and Characterization of Polymers For Optical Waveguides	23
2.1 I ntroduction	23
2.1.1 Guide as Negative Photoresist	23
2.1.2 S ynthetic Control	23
2.1.3 P olymer Composition	24
2.2 E xperimental	27
2.2.1. G eneral Methods	27

2.2.2 Reag	2.2.2 Reagents & Materials		
2.2.3 Prep	aration of Materials for Polymer Synthesis	28	
2.2.3.1	Purification of Benzoyl Peroxide (BPO)	28	
2.2.3.2	Synthesis of 4-hydroxystyrene (4HS or <i>paraTxx</i>)	29	
2.2.4 P oly	mer Synthesis	30	
2.2.4.1	Synthesis of Guiding Polymer Precursor, Styrene- co-pentafluorostyrene (cop1Txx)	30	
2.2.4.2	Synthesis of Guiding Polymer, Styrene- <i>co</i> -penta- fluorostyrene- <i>co</i> -[4-styren-4'-yl-2,3,5,6- tetrafluorophenylether] (<i>terTxx</i>)	31	
2.2.4.3	Synthesis of Buffer Polymer Precursor, 4-fluoro- styrene- <i>co</i> - pentafluorostyrene (<i>cop2Txx</i>)	31	
2.2.4.4	Synthesis of Buffer Polymer, 4-fluorostyrene- <i>co</i> -pentafluorostyrene- <i>co</i> -[4-styren-4'-yl-2,3,5,6-tetrafluorophenylether] (<i>bufTxx</i>)	32	
2.2.4.5	Synthesis of Cladding Polymer, Glycidyl methacrylate- <i>co</i> -styrene- <i>co</i> -pentafluorostyrene (<i>cladTxx</i>)	32	
2.3 R esults &	Discussion	33	
	nuated Total Reflection Fourier Transform Infrared ATR FT-IR) Spectroscopy	34	
2.3.1.1	Characterization of Polymers and Precursors	34	
2.3.1.2	Analysis of Reproducibility	38	
2.3.2 Gel l	Permeation Chromatography (GPC)	39	
$2.3.3^{-1}$ H N	luclear Magnetic Resonance (NMR) Spectroscopy	41	
2.3.4 T her	mal Analysis	45	
2.3.4.1	Thermal Gravimetric Analysis (TGA)	45	
2.3.4.2	Differential Scanning Calorimetry (DSC)	47	
2.4 C onclusion	on	49	
CHAPTER 3	Waveguide Lithography and Fabrication	52	
3.1 I ntroducti	on	52	
3.1.1 T he	Fabrication Process	52	

3.1.2 D irect Lithographic Patterning	
3.1.3 McGill University Microfabrication Facility	55
3.2 E xperimental	55
3.2.1 G eneral Methods	55
3.2.1.1 Sample Handling	55
3.2.1.2 Spincoating	56
3.2.1.3 B aking	56
3.2.1.4 P lasma Oxidation	56
3.2.2 Reagents & Materials	56
3.2.3 S ubstrate Preparation	57
3.2.3.1 P iranha Cleaning	57
3.2.3.2 Functionalization with Triethoxyvinylsilane	57
3.2.4 Application of Buffer Layer	58
3.2.5 Application of Guiding Layer and Photolithography	59
3.3 Results & Discussion	62
3.3.1 S ubstrate Functionalization	63
3.3.2 Application of Buffer Layer	63
3.3.3 Application of Guiding Layer	64
3.3.3.1 Calibration of Layer Thickness	64
3.3.3.2 Optimization of UV Exposure	66
3.3.3.3 Optimization of Etching Conditions	68
3.3.3.4 Refractive Index Analysis	73
3.3.4 Application of Buffer Layer as Cladding	73
3.3.5 E nd-Coupling in Lithographic Structures	74
3.5 Conclusion	77
Summary	77

CHAPTER 1:

INTRODUCTION AND BACKGROUND

There is currently a worldwide demand for higher performing telecommunications networks with greater bandwidth and faster information transfer. These needs can be met w ith higher pe rforming materials f or network components. Optical d ata transmission, the basis of the telecommunications network, requires a wide array of optical and electro-optical devices to gui de and manipulate light signals. Fiber-type waveguides can support guided waves for up to hundreds of kilometers with low loss. While glass fibers, the current standard, are sufficient for transferring information over long path lengths they are not a ppropriate f or high-density waveguiding c ircuitry because their fragility makes such structures difficult to produce. Polymers have potential as optical materials for such components.

Carefully designed polymers offer the promise of durability and superior efficiency in data transfer. Current fiber optics transmits telecommunications information at 1.55 µm because it is found to be the optimal wavelength for propagation within glass, exhibiting minimal loss. New materials must adapt to this pre-established specification and also prove capable of being fabricated into appropriate device structures. The focus of this thesis is the synthesis and development of polymers for optics and their processing to form optical waveguides.

1.1 OPTICAL WAVEGUIDES

The buried waveguide is basic to many integrated optical devices, including the optical amplifier. In general, a waveguide is a material which regulates light wave propagation via total internal reflection. For reflection to occur, the index of refraction of the waveguide must be higher than that of its surroundings. This is most easily illustrated in the case of the slab waveguide, represented in Figure 1.1.

To produce a buried waveguide, polymer layers are deposited onto a solid substrate by spin-coating. First a buffer layer covers the substrate making a suitable surface for the guiding core layer, isolating the core from undesirable optical interactions with the substrate. The core is applied, followed by a protective cladding layer whose optical properties are selected so as to confine the optical field guided by the core.

Spin-coating is one of the techniques used to deposit polymer films. Spin-coating requires a high precision tool (the coater) equipped with a vacuum chuck to hold the substrate which is coated with a solution of the polymer. Digitally programmed spin sequences control the angular velocity and time during which the coating process takes place. The angular velocity overcomes the adhesive force of the solution to the substrate, depositing a thin coat of polymer. During the spin phase, the carrier solvent rapidly evaporates causing the temperature of the solution to fall. Polymer solubility usually decreases with decreasing temperature and solvent content, and so the polymer deposits rapidly as a nonequilibrium film from solution. Acceleration, maximum velocity, time, solvent and concentration all influence the final thickness and quality of the deposited film.²

For t elecommunications a pplications, c ore polymers must have a n index of refraction, n, close to that of optical fiber to which they are coupled in order to achieve correct modal field overlap so that power can be coupled from one medium to the other. The value of n relates the velocity of light traveling through a vacuum, c, to the velocity of light traveling through a medium, c_{medium} (Equation 1.1). In a ray optics approximation, Snell's Law (Equation 1.2) describes the relationship between n and the angle of incidence of light passing through the boundary of two isotropic media.

$$n = \frac{c}{c_{\text{medium}}} \tag{1.1}$$

$$n_{\rm A}\sin\theta_{\rm A}=n_{\rm B}\sin\theta_{\rm B}\tag{1.2}$$

1.1.1 THEORETICAL DESCRIPTION OF WAVEGUIDING

The ray-optics description of waveguiding considers a single ray of light that is reflected within a medium, as shown in Figure 1.1. The interfaces above and below the core are parallel to the *x-y* plane and the wave is propagating in the *x* and *z* directions.

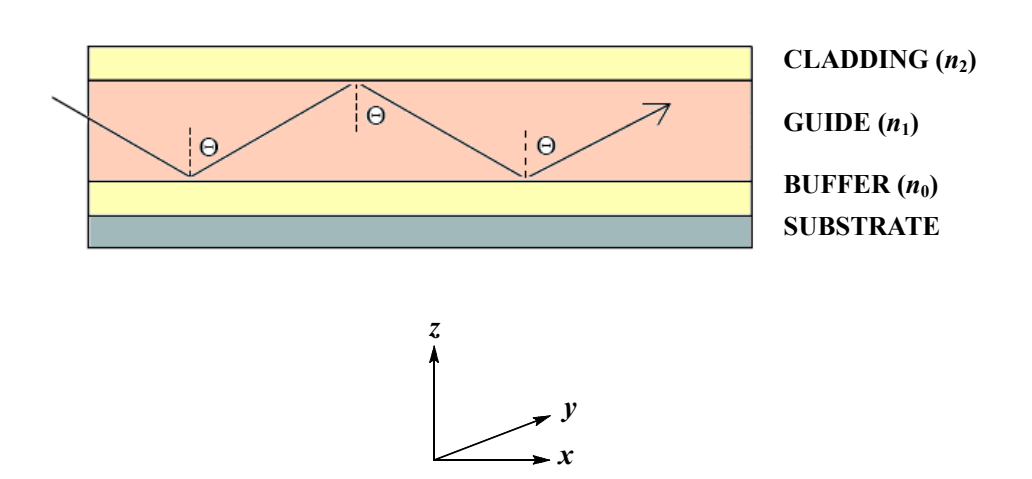


FIGURE 1.1 Representation of internal reflection within an isotropic slab waveguide in two dimensions. The a rrow i ndicates a r ay of l ight propagating t hrough t he w aveguide c ore, r eflecting f rom t he boundaries of the guiding material as described by Snell's Law (Equation 1.2).

The indices of refraction of the three media are n_0 , n_1 , and n_2 , for the buffer, guide and cladding, r espectively. Light pr opagating t hrough a n i deal, c ore with an isotropic refractive i ndex will not remain within the c ore boundaries unless the a ngle of incidence, θ , exceeds the following critical value:

For the cladding/core interface:

$$\theta > \sin^{-1}\left(\frac{n_2}{n_1}\right) \tag{1.3}$$

For the core/buffer inteface:

$$\theta > \sin^{-1}\left(\frac{n_0}{n_1}\right) \tag{1.4}$$

This relationship can also be interpreted as the requirement that n_1 , the refractive index of the core, must be higher than the refractive indices of the buffer and cladding layers, n_0 and n_2 , to ensure reflection back into the core. In fiber-type waveguides, the buffer and cladding are enclosed in one coating surrounding the cylindrical fiber. This is us ually c overed w ith a n a dditional i nsulating a nd a rmored c ladding l ayer f or environmental protection.

The propagation of a light wave in the x and z directions through a slab waveguide in the x-y plane (Figure 1.1) has a phase constant, β , that can be broken into components b_1 and kn_1 (Figure 1.2). Here, k is a wavenumber defined as the ratio of a ngular frequency, ω , to the velocity of light in a vacuum, also described as the propagation constant of free space. The variable b_1 is the z-component of the wavenumber and n_1 is the refractive index of the waveguide.³

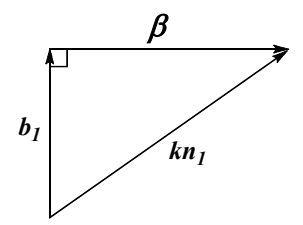


FIGURE 1.2 Components of β , Propagation Constant of a Wave.

$$\beta = k n_1 \sin(\theta) \tag{1.5}$$

$$N = \frac{\beta}{k} = n_1 \sin(\theta) \tag{1.6}$$

$$k = \frac{\omega}{c} \tag{1.7}$$

The mode index, N, is called the effective refractive index. A guided mode, m, is the periodic path a light wave will travel through a waveguide. Modes have unique profiles and are conventionally numbered $m = 0, 1, 2 \dots$, where m counts the number of nodes. The lowest order mode corresponds to the highest value of N and the smallest

angle θ . The phase constants of different guiding modes are denoted as β_m and have corresponding angles θ_m which must be less than the critical angle, θ_c . The number of guided modes depends on the film thickness, W, the wavelength of radiation, and the indices of refraction for the core and its surrounding layers. Assuming waves do not penetrate the surrounding layers, the angles corresponding to guided modes and the number of allowed guided modes, m_{max} , for a medium can be determined as follows:

$$\theta_m = \frac{(m+1)\pi}{n \, kW} \tag{1.8}$$

$$m_{\text{max}} = \left(\frac{kW\theta_c}{\pi}\right) - 1 \tag{1.9}^4$$

While ray-optics gives a reasonable depiction of waveguiding, the electromagnetic wave description is required for a complete representation. The electromagnetic field distribution within a waveguide can be viewed as the superposition of two plane waves: those of the electric and magnetic fields. In rectangular coordinates, waves propagate over time, t, as:

$$\exp\left[i\omega t \pm ik_{xj}x \pm ik_{yj}y \pm ik_{zj}z\right]$$
 (1.10)³

with j = 0, 1, 2 representing the buffer, guide, and cladding, respectively. Here k is the ratio of a particular directional component of angular frequency to the velocity of light in a vacuum. This expression can be rearranged into the wave equation of an isotropic medium, knowing the directional components and the operator, k.

$$\left(\frac{\partial^2}{\partial x^2} + \frac{\partial^2}{\partial y^2} + \frac{\partial^2}{\partial z^2}\right) E_j = -k^2 n_j^2 E_j$$
 (1.11)

Here E_j is the electric field. Replacing E_j by H_j gives the corresponding equation of magnetic field. Maxwell's equations sepa rate the electric and magnetic field components into two sets, the Transverse Electric (TE) and Transverse Magnetic (TM). TE has field components E_{xj} , H_{xj} and H_{zj} while TM has field components E_{xj} , E_{zj} and H_{yj} . Solving Maxwell's equations yields expressions which relate the phase constants of allowed modes, β , to film thickness.³ There are multiple solutions, each representing a different guided mode. Here, β appears as the eigenvalues of these modes.

for TE:
$$\tan(b_1 W) = \frac{b_1(p_0 + p_2)}{(b_1^2 - p_0 p_2)}$$
 (1.12)

for TM:
$$\tan(b_1 W) = \frac{b_1 \left[(n_1 / n_2)^2 p_0 + (n_1 / n_2)^2 p_2 \right]}{b_1^2 - (n_1^2 / n_0 n_2)^2 p_0 p_2}$$
 (1.13)

where:
$$b_1^2 = k^2 n_1^2 - \beta^2$$
$$p_{0,2}^2 = \beta^2 - k^2 n_{0,2}^2$$

While mode selection and the use of Snell's Law are straightforward examples of ray-optics principles, real films are typically anisotropic, causing them to be bi- or multi-refringent. The interaction between an electromagnetic light wave and polarizable materials complicates this description, decreasing the speed of the wave and resulting in a higher index of refraction (Equation 1.1).

Polarization dependence in waveguide materials may be caused by changes in the orientation of functional groups within the material and atomic displacements.⁵ In an applied electric field, molecules with permanent dipoles may shift to a lign with the field. A tomic bonds within the molecules are susceptible to stretching and bending under the same conditions. If the structure of the waveguide material itself is relatively immobile, high electronic mobility of its molecules will still contribute to polarizability,

increasing interaction with an applied electric field. This is of ten observed for π -systems, such as aromatics.

As in the ray optics approximation, the number of guided modes in the electromagnetic description depends on three variables: film thickness, wavelength radiation, and the indices of refraction for all three media. It is important to note that while field intensity distributions within the waveguide layer are sinusoidal, they decay exponentially beyond the interface in the substrate and superstrate.

Prism coupling, grating coupling, and end-coupling are common methods to excite the modes of a waveguide. In prism coupling, polarization of the incident ray is preserved and a percentage of the incident intensity is transferred into the waveguide when $n_{\text{prism}} \ge n_1$. Experimentally, a prism is pressed to the film surface through which light is refracted. There exists a small gap between the prism and the film due to dust or, most often, to surface irregularities. When the *x*-direction of the propagation constant of the beam through the prism matches one of the propagation constants, β , of the film, then the beam enters. Hence, for a single wavelength laser, individual modes can be selected by changing the angle of incidence (Equation 1.8). A grating coupler can be used to select specific incident angles without adjusting the laser position or to select specific wavelengths from a broad-spectrum light source. This permits the selection of particular allowed modes. As with all coupling techniques, this phase matching is essential to initiate light propagation in a waveguide.

Once lithographically or laser written structures have been patterned, it becomes difficult to excite them by prism coupling. Optical fibers are most often used instead, primarily for end-coupling in fiber-type or buried waveguides. Rather than enter from the top of the waveguide, light is input from the clean, flat end surface of a fiber strand. Coupling then relies on modal field overlap between the light emerging from the fiber and the allowed modes of the buried waveguide.

1.1.2 OPTICAL LOSS

Optical loss is the amount of optical power lost as light is transmitted through an optical device. For telecommunications and data communications optical devices it is especially important that the material have low optical loss in the regions of 1.3 μ m and 1.55 μ m. These regions are know n a s t he opt ical w indows f or da ta- and telecommunications. It is important that light at these wavelengths experience little to no loss so that signals can be fully transmitted.

Scattering loss at the datacom and telecom wavelengths is primarily attributed to defects or b ends in a waveguide. I mpurities such as dust or processing solvents trapped during fabrication, surface irregularities, and physical flaws such as cracking or buckling can cause irregular light scattering.⁷ Defects at the molecular level contribute to anisotropy, which can produce birefringence.

Birefringence can be v iewed as a 1 oss mechanism through the polarization dependence of propagation. Polarization dependence arises from variations in the indices of refraction encountered by the TE and TM modes. These indices, n_{TE} and n_{TM} , have different electromagnetic field distributions according to Maxwell's equations.³ Birefringence is denoted by Δn , and can be defined simply as the calculated difference between n_{TE} and n_{TM} . Often an effect of inherent material polarizability, birefringence also occurs when a waveguide is submitted to mechanical stress.⁸

Waveguides can experience a bsorption loss c aused by c oupling to molecular vibrations of the host guiding material. Carbon-hydrogen, oxy gen-hydrogen, and nitrogen-hydrogen bond pairs e ach have vibrational overtones that fall in the telecommunications optical window, absorbing signal intensity. To understand this, we can write a simple expression for the vibrational frequencies, v, which relates the reduced mass, μ , of the bonded atoms and the force constant, f,

$$v = \frac{1}{2\pi} \sqrt{\frac{f}{\mu}} \tag{1.14}$$

In or ganic polymers, the low reduced mass of C-H results in high vibrational frequencies and therefore lower absorptive wavelengths. Substituting a heavier atom for hydrogen in the bond pair increases the vibrational frequencies, partially shifting the stronger overtones out of the optical window. This will be further discussed in Section 1.2.2.

1.1.3 PROCESSING AND FABRICATION

Planar w aveguides c ontain a c omplete gui ding layer t hrough w hich l ight m ay propagate. For optical devices, it is more common that the core polymer take the form of a rib waveguide, which mimics an "optical wire". The core material is formed into one or many straight ridges before the cladding layer is applied, such that it is covered on all sides by lower refractive index material. This type of waveguide is represented in Figure 1.3. Here, a strip of guiding polymer, the "rib", sits on a layer of buffer polymer which lies on a substrate. The entire device is covered with a protective cladding layer. The c ore p olymers f or r ib w aveguides a re p atterned e ither by c onventional m ask lithography or laser self-writing. In both cases, extraneous polymer is removed after waveguide formation before the structure is covered with cladding.

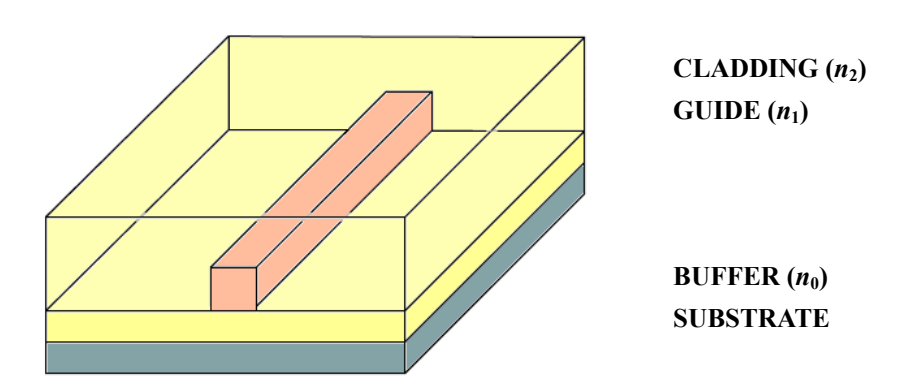


FIGURE 1.3 Representation of a buried rib waveguide.

Fabrication of waveguides by phot olithography i s pe rformed in multistep processes. The width of the waveguides is usually established beforehand by numerical modeling and calculations which can be used to define the dimensions of the mask to be used. For photoresist-based patterning, a layer of photoresist material is deposited over the core polymer layer. Light is passed through the lithographic mask placed over the surface to project an image of the waveguide shape, chemically altering the surface such that only the unaffected portions are removed with an appropriate solvent. The newly exposed polymer surface is then stripped by reactive ion etching (RIE), leaving the photoresist-covered areas untouched. The waveguide ribs are revealed by removal of the remaining photoresist. This kind of resist is called a negative photoresist.

Direct lithographic patterning, the focus of this thesis, requires a polymer core which is modified upon light exposure. The photoinitiation process is either the result of a bimolecular process requiring an initiator molecule or decomposition of a single excited molecule. Often, patterning is achieved via photoinitiated crosslinking. The pattern is created directly by light exposure through a mask and the unexposed regions are washed away with an appropriate solvent.

Photoinitiated crosslinking is a lso commonly used to create rib waveguides by self-writing with a laser beam. In this method, light is passed through the core polymer initiating chemical change. The remaining portion is a gain removed with a solvent. This technique is advantageous for its processing speed and rapid prototyping. Laser writing can also produce waveguides as I ong as seve ral meters on flexible plastic rolls. ¹¹ The primary disadvantages of I aser writing are sidewall roughness, size resolution, and the inability to form complicated waveguide components, such as Y-shaped splitters.

1.2 POLYMERS IN OPTICS

Most devices used in optics, including lenses, splitters and transformers, can be constructed from polymers. It is important that polymeric devices allow long-range interactions be tween l ight a nd t he opt ical polymer t o m inimize s ignal loss. T his becomes especially significant in the design of polymeric fibers to replace glass as the chief material in telecommunications. In this form, durability and loss can be measured to assess the suitability of a material for long-range optics. In this thesis, the waveguide itself is explored as an optical device.

1.2.1 CHARACTERISTICS FOR OPTICAL APPLICATIONS

Polymers h ave a n e normous va riety of tunable properties, which makes them desirable for optical purposes. M inor changes to their composition or synthesis can adjust molecular weight distributions, transparency and refractive index to maximize device efficiency. Polymers r eplacing glass d evices require a cer tain a mount of mechanical strength in order to withstand stress and strain from their positioning. Long-haul waveguiding devices such as optical cables also require material flexibility. Copolymerization can achieve these characteristics by combining the best qualities of two or m orem onomer types. The preparation of polymers w ith particular characteristics also requires careful consideration of many processing variables to achieve the desired composition and function. While this certainly presents more challenges to production than the current glass-based optical systems, it also allows the fine-tuning of polymer properties by simple processing conditions such as thermal control, reagent ratios, and reaction time, or by changing the molecular composition of the monomers.

The durability of polymers is evaluated by t esting properties such as thermal stability. Changes in composition over time, including depolymerization, can result in degradation leading to signal reduction or complete product failure. As previously

mentioned, guided wave optics depends on the core polymer having a higher index of refraction t han i ts s urroundings. I f de gradation a lters t his c ondition l ight c annot propagate a nd i nformation i s lost.² Transparency i s hi ghly i mportant f or opt ical polymers. The internal organization of polymer s trands w ithin w aveguiding media contribute to their transparency as well as other optical properties. Modifications to monomer composition or processing c onditions can alter this organization, reducing transmission loss.

Polymer hom ogeneity is i mportant f or optical a pplications. P hysical flaws in optical devices can create scattering losses great enough to destroy function. While bubbles or cracks may result from poor processing reproducibility or low molecular weight f ractions, most defects c and be a voided by a ttentive purification of the monomeric starting materials and careful polymerization with control of molecular weight. Production must begin with highly purified monomers as well as initiators and regulators, if they are required. Many monomers are stored in the presence of inhibitors to prevent early polymerization which must be removed prior to use. To minimize defects in industry, device processing steps are sometimes performed in sequence by a costly self-contained machine. ¹²

The family of polymers synthesized for the experiments described in this thesis was selected for a variety of controllable chemical and physical properties which are important in the formation of waveguides. These include reduced optical loss and high transmittance, particularly at the wavelengths where they are to guide.

1.2.2 VIBRATIONAL LOSS IN POLYMERS

As discussed in Section 1.1.2, most polymers experience high optical loss at IR wavelengths due to the vibrational absorption by carbon-hydrogen bonds. In this thesis, we are particularly concerned with vibrations of the C-H bonds in our styrene-based polymer waveguiding s ystems. ¹³ Theoretical ov ertone a bsorption w avelengths f or aliphatic C-H, carbon-deuterium, and carbon-fluorine bond pairs are compared in Table 1.1. The symbol v_f stands for the fundamental vibration while v_n denotes the $(n-1)^{th}$

overtone of order n.¹⁴ Note that C-H has 1st and 2nd overtones near the optical window while C-F has its relatively weaker 4th, 5th and 6th overtones in the same region. Higher order overtones are further from the fundamental vibration and therefore less absorbing. Aromatic o vertones o ccur at som ewhat higher wavenumber than those due to the aliphatic substituents.

Owing to differences in molecular s tructure, vibrational w avelengths f or compounds containing these bond pairs will vary somewhat from the calculated values in Table 1.1.

TABLE 1.1 Vibrational Wavelengths, λ , for Selected Bond Pairs Determined by Theoretical Calculations. ¹⁴ (NOTE: Vibrations relevant to absorption loss in the optical window appear in *italics*.)

VIBRATION	λ (C-H) (nm)	λ (C-D) (nm)	λ (C-F) (nm)
v_f	3390	4484	8000
v_2	1729	2276	4016
v_3	1176	1541	2688
v_4	901	1174	2024
<i>v</i> ₅	736	954	1626
v_6	627	808	1362
v_7	549	706	1171

For the waveguides produced in this thesis research, we must consider vibrational loss in polystyrene and analogous structures. Hydrogen atoms on the aromatic ring of styrene c an be substituted with fluorine in order to shift vibrational overtones, as suggested in Table 1.1. In styrene, the first overtone of the ring C-H stretching vibration falls into the 1.55 µm optical window at approximately 1.61 µm, causing unwanted

absorption.¹³ For pentafluorostyrene, only the very weak 5th vibrational overtone of C-F in pentafluorostyrene falls into the telecommunications window, making it less absorptive than styrene in this region.

FIGURE 1.4 (a) Styrene; (b) Pentafluorostyrene

One drawback to the use of highly fluorinated materials for waveguide formation, is that they often show very poor adhesion and wetting properties and low solubility,. Therefore, a tradeoff must be made between optical loss due to vibrational overtones and ease of polymer processing; poly(pentafluorostyrene) homopolymer cannot be used on its own as an optical material. We obtain a compromise through copolymerization in order to combine the low IR absorption of pentafluorostyrene with the desirable physical and chemical properties imparted by styrene. This is the rationale behind the chemical design of the guiding polymer developed in this thesis research.

1.2.3 REVIEW OF POLYMERS FOR OPTICAL WAVEGUIDES

A variety of polymer systems have investigated for optical applications over the last two decades. Glass fiber-optic cables have waveguide cores comprised of silica and exhibit near-negligible optical loss of 0.15 dB/km at 1.55 μ m. New materials for short-path optical devices should minimally exhibit optical loss below 0.5 dB/cm at 1.55 μ m, and can be deemed "high performance" if they exhibit attenuation near or below 0.1 dB/cm a nd glass t ransition temperature, T_g , above 300 °C. T_g is the temperature at which an ordered material transitions from a brittle to an amorphous state and it a measure of thermal stability.

The first polymers used for optics were limited in their applications by the type of plastics available. These were often active small-molecule waveguides contained in polymer cladding. Manufacturing and material constraints meant only devices with low performance requirements could be created.² For example, electrooptic modulators were produced by hos ting methylnitroaniline molecules in metastable orientation in poly(methylmethacrylate). Such systems never advanced because the lossy devices showed unsatisfactory modulating activity when ordered guest molecules relaxed to random orientations over time. Presently there is a wide array of polymer systems under investigation.¹⁵

1.2.3.1 Polysiloxanes

Silica fibers are currently the most efficient medium for long distance data transfer. Although glass is impractical for hi gh-density optical c ircuitry, s ilica-based waveguides aim to take advantage of the mechanical and thermal stability of a siloxane network. Siloxanes are affected by vi brational loss from O-H bond pa irs, which are minimized by careful processing.

Deuterated pol y(phenylsiloxane), c ontaining a s iloxane b ackbone, ha s be en formed by hydrolysis and polycondesation of deuterated phenyltrichlorosilane (Figure 1.5a). Although it is common to reduce absorption losses in polymers by substituting heavier atoms for hydrogen, this monomer proves to be an exception. Its absorption loss is actually increased from the deuterated form at 1.55 μ m as an absorption peak shifts directly into the telecommunications window.

To form devices from deuterated poly(phenylsiloxane), the material is spin-coated to produce a thin film and the device is waveguide is patterned with the assistance of a photoresist and reactive ion etching (RIE). These materials have exhibited refractive indices of 1.5365 at $1.3~\mu$ m and 1.5345 at $1.55~\mu$ m, and attenuation as low as 0.17 dB/cm a nd 0.43 dB /cm for t he da ta- and t elecommunication w avelengths, respectively. ¹⁷ Deuterated phe nyltrichlorosilane ha s be en c opolymerized w ith methyltrichlorosilane, also by hydrolysis and polycondensation, with varying monomer ratios, e xpanding t he network of s ilicone and pr oviding a ttenuation a s l ow a s

0.23dB/cm at 1.55 μ m and T_g greater than 300 °C for all compositions. ¹⁸

$$D \longrightarrow D$$

$$D \longrightarrow$$

FIGURE 1.5 (a) Deuterated phenyltrichlorosilane; (b) Methyltrichlorosilane

1.2.3.2 Polyacrylates

The simplest acrylate polymer, poly(methyl methacrylate) (PMMA), has typical optical loss in the range of 1 dB/cm but has been reported with attenuation as low as 0.25 a nd 0.75 dB /cm at 1.3 a nd 1.55 μ m, r espectively, f or di fferent pr eparation techniques. ¹⁹ The phot ochemical pro cessing of m ethyl methacrylate t o P MMA is characterized by l ow i nternal s tress a nd hi gh uniformity⁹, a nd P MMA w aveguide structures can be formed by direct lithographic patterning on silica with optical losses of 1 dB /cm at the telecom wavelength. PMMA is also highly scratch resistant and resistive to damage from ultraviolet light, making it appropriate for lower wavelength or broad-spectrum devices. ²⁰

A major di sadvantage is its poor thermal stability, with T_g of various PMMA waveguide pr eparations r anging f rom 85 t o 115 ° C. C ommercial ha logenated acrylate-based polymers have been prepared with no improvement to propagation loss (1.2 dB/cm at 1.55 μ m) but T_g as high as 365 °C.²¹

Absorption loss in has been reduced by de uteration or halogenation in many acrylate-based polymers. Perdeuterated poly(methyl methacrylate) (d-PMMA) multimode waveguides have been formed by photoresist lithography and oxygen RIE. The waveguides exhibited greatly improved attenuation at 1.3 μ m, from 0.31 to 0.073 dB/cm, owing to the shift of vibrational absorption in the absence of C-H bonds. This same shift resulted in a loss increase at 1.55 μ m, from 0.83 to 1.35 dB/cm, as one of the vibrational overtones fell directly in the telecommunications window.

Halogenated a crylate t erpolymers of pe ntafluorophenylacrylate, pe ntafluoro-

phenylmethacrylate and tetrachloroethylacrylate (Figures 1.6b-d) have been developed for direct photolithographic patterning. A refractive index range of 1.464-1.518 at 1.3 μ m c an be a chieved by a djusting t he c omponent r atios of t he t erpolymer. ²³ The minimum optical loss reported was 0.2 dB/cm at 1.3 μ m and 0.7 dB/cm at 1.55 μ m, but thermal st ability was poor, falling in the s ame glass t ransition range as P MMA waveguides. ²⁴

FIGURE 1.6 (*a*) deuterated methyl methacrylate (d-MMA) (*b*) tetrachloroethylacrylate; (*c*) pentafluorophenylacrylate; (*d*) pentafluorophenylmethacrylate.

1.2.3.3 P olyimides

While pol yimides exhi bit exc ellent mechanical and thermal st ability, they are generally unacceptable for optical devices owing to high signal losses from scattering and pol arization di spersion loss due to the bi refringence. Optical a nisotropy a rises because of internal ordering of the polymer structure in the form of aromatic stacking, while losses are enhanced because of the formation of water during polymerization, which also r esults in t iny hole defects (scattering centers) in the waveguide. Halogenation appears to help in reducing scattering as well as vibrational losses from the organic components and water. Steric hindrance from trifluoromethyl groups added to acrylate polymer linkages in certain polyimides force the polymer chains out of their typical planar orientation. Device fabrication from fluorinated polyimides requires photoresists and R IE. The r esulting devices exhibit h igh bi refringence ow ing to polarization of the still somewhat ordered structures.

Polyimide-silica hybrid materials have been made by sol-gel reactions to prepare planar w aveguides on s ilicon s ubstrates. ²⁶ Waveguides m ade f rom t he polyimide

pyromellitic dianhydride-co-oxydianiline (PMDA-ODA) alone exhibit optical loss of 2.9 dB/cm at $1.31 \mu m$, which is lowered as much as 1 dB/cm in the its hybrid with silica owing to the reduced C-H bond content.

FIGURE 1.7 Pyromellitic dianhydride-co-oxydianiline (PMDA-ODA)²⁶

1.2.3.4 F luorinated Arene Polymers

Aromatic r ings c ontained polymeric de vice s tructures like thos e f rom poly(phenylsilane) and poly(phenylsiloxane) presented in Section 1.2.3.1 lend optical materials relatively low attenuation and improved thermal stability. Polystyrene has high electronic absorption loss in UV wavelengths but relatively low loss in the infrared, making it a candidate starting material for optical polymers for telecommunications devices. ²⁰ It is also preferred over other polymers for its low hygroscopicity coefficient. Polystyrene absorbs one-tenth less water than PMMA in humidity tests. Nevertheless, polystyrene is still too lossy for optical communications and because it is a l inear polymer, it lacks the properties (solvent resistance and photopatternability) required for integrated optics device fabrication.

Fluorinated pol y(arylene e ther) uni ts ha ve b een de signed w ith c rosslinkable (phenylethynl)phenol e nd gr oups a s a pho topatternable w aveguiding m aterial, FPAE-PEP.²⁷ These pol ymer w aveguides are s ubmitted t o a relatively h igh c uring temperature of 320 °C for two hours and exhibit loss less that 0.2 dB/cm at 1.55 μ m and a birefringence, Δn , of 0.0078.

FIGURE 1.8 Fluorinated poly(arylene ether) with (phenylethynl)phenol end groups (FPAE-PEP)²⁷

Adjustments t o the F PAE-PEP pol ymer s tructure p roduced w aveguides w ith reduced birefringence by improving molecular flexibility and lowering the waveguide curing temperature. C arbonyl groups were introduced be tween the fluorinated ring structures in the polymer backbone and the end group was replaced by *meta*-substituted ethynlphenol (E P), facilitating easier c rosslinking. ²⁸ The r esulting f luorinated poly(ether ketone), FPEK-EP, exhibited $\Delta n = 0.0023$ with curing for 2 hours at 250 °C and even further reduced birefringence to $\Delta n = 0.0014$ with curing for 4 hours at 235 °C. These improvements come at some cost to thermal stability, as T_g fell slightly to 460 °C under nitrogen and optical loss rose to 0.5 dB/cm at 1.55 μ m.

$$\begin{bmatrix}
F & F & O & F & F_3C & CF_3 \\
F & F & F & F
\end{bmatrix}$$

FIGURE 1.9 Fluorinated poly(ether ketone) with m-ethynylphenol end groups (FPEK-EP)²⁸

Copolymers of pentafluorostyrene (Figure 1.4a) and glycidyl methacrylate (Figure 1.10) ha ve be en d eveloped f or u se i n w aveguides pho toprinted by f ree-radical crosslinking. The copolymer composition can be varied to precisely control refractive index and the resulting single mode waveguides have attenuation as low as 0.42 dB/cm at 1.55 μ m with $\Delta n = 0.0004$.²⁹

FIGURE 1.10 Glycidyl methacrylate

This combination achieves a balance between the behaviors of the individual polymer families in the presence of solvents. Polystyrenes experience swelling while acrylates are susceptible to shrinkage and cracking.

These qualities were considered when preparing polymers for the waveguides described in this thesis. Glycidyl methacrylate was included with fluorinated polystyene in the cladding polymer to reduce solvent swelling during device processing. Swelling would exert mechanical stress on the waveguide core resulting in structure deformation and scattering loss.

The following c hapters de scribe our r esearch in the s ynthesis of a variety of polymers for optical waveguides and methods to fabricate optical devices from them.

¹ L. Eldada, R. Blomquist, L.W. Shacklette, M.J. McFarland, *Opt. Eng.*, **39**, 596-609 (2000).

- ⁴ M.J. Zwanenberg, *X-Ray Waveguiding Studies of Ordering Phenomena in Confined Fluids*, Ph.D. Thesis, University of Amsterdam, 2001.
- ⁵ C.H. Henry, G.E. Blonder, and R.F. Kazarinov, *IEEE J. Lightwave Technol.*, **7**(10), 1530-1939 (1989).
- ⁶ T. Kanigan, *Integrated Optics Spectroscopy of Polymer Thin Films*, Ph.D. Thesis, McGill University, 1995.
- ⁷ L.W. Shacklette, R. Blomquist, J.M. Deng, P.M. Ferm, M. Maxfield, J. Mato, and H. Zou, *Adv. Funct. Mater.* **13**, 453 (2003).
- ⁸ D.W. van Krevelen, *Properties of Polymers*, 3rd Ed., Elsevier: Amsterdam, 1990.
- ⁹ L. Eldada and L.W. Shacklette. *IEEE Quantum Electronics*. **6**, 54 (2000).
- N.S. Allen et al., Eds., Current Trends in Polymer Photochemistry, Ellis Horwood: New York, 1995. p40.
- ¹¹ L. Eldada, X. Chengzeng, K.M.T. Stengel, L.W. Shacklette, and J.T. Yardley, *J. Lightwave Technol.*, **14**, 1704 (1996).
- ¹² N. Lekishvili *et al.*, *Polymers and Polymeric Materials for Fiber and Gradient Optics*, VSP: Utrecht, 2002. pp26-30.
- ¹³ H. Ma, A.K.-Y. Jen, and L.R. Dalton, *Adv. Mater.*, **14**, 1339 (2002).
- A. Rousseau, B. Boutevin, and D. Bosc in *Proceedings of the First Plastic Optical Fibres and Application Conference*, *Paris*, 1992, IGI Europe: Boston, MA, 1992. p33-37.
- ¹⁵ L. Eldada, *Proc. SPIE*, **4642**, 11 (2002).
- ¹⁶ M. Usui, S. Imamura, S. Sugawara, S. Hayashida, H. Sato, M. Hikita, T. Izawa, *Electron. Lett.*, **30**, 958-959 (1994)

² D.J. Wise, *Photonic Polymer Systems: Fundamentals, Methods, and Applications*, Marcel Dekker, Inc.: New York, 1998; Early applications: p526; Spin-coating: p738.

³ P.K. Tien, *Rev. Mod. Phys.*, **49**, 361 (1977).

¹⁷ M. Usui, M. Hikita, T. Wantanabe, M. Amano, S. Sugawara, S. Hayashida, S. Imamura, *J. Lightwave Technol.*, **14**, 2338-2343 (1996).

¹⁸ S. Toyoda, N. Ooba, M. Hikita, T. Kurihara, S. Imamura, *Thin Solid Films*, **370**, 311-314 (2000).

¹⁹ R.A. Norwood, R. Gao, J. Sharma, C.C. Teng, *Proc. SPIE*, **4439**, 19-28 (2001).

²⁰ D.L. Keyes, R.R. Lamonte, D. McNally and M. Bitritto, "Polymers for Photonics", *Photonics Spectra*, **10**, 131 (2001).

²¹ L. Eldada, S. Yin, R.A. Norwood, J.T. Yardley, *Proc. SPIE*, **3234**, 161-174 (1998).

²² R. Yoshimura, M. Hikita, S. Tomaru and S. Imamura, *J. Lightwave Technol.*, **16**, 1030 (1998).

²³ M. Jöhnck, L. Müller, A. Neyer, J.W. Hofstraat, Eur. Polym. J. 2000, 36, 1251-1264.

²⁴ M. Jöhnck, L. Müller, A. Neyer, J.W. Hofstraat, *Polymer* **1999**, *40*, 3631-3640.

²⁵ J. Kobayashi, T. Matsuura, S. Sasaki, T. Maruno, *Appl. Opt.*, **37**, 1032-1037 (1998).

²⁶ C.-C. Chang, W.-C. Chen, *Chem. Mater.*, **14**, 4242-4248 (2002).

²⁷ H.-J. Lee, E.-M. Lee, M.-H. Lee, M.-C. Oh, J.-H. Ahn, S.G. Han, H.G. Kim, *J. Polymer Sci. A*, **36**, 2881-2887 (1998).

²⁸ H.-J. Lee, M.-H. Lee, M.-C. Oh, J.-H. Ahn, S.G. Han, *J. Polymer Sci. A*, **37**, 2355-2361 (1999).

²⁹ C. Pitois, S. Vukimirovic, A. Hult, D. Wiesmann, M. Robertsson, *Macromolecules*, **32**, 7817-7821 (1999).

CHAPTER 2:

PREPARATION AND CHARACTERIZATION OF POLYMERS FOR OPTICAL WAVEGUIDES

2.1 INTRODUCTION

2.1.1 GUIDE AS A NEGATIVE PHOTORESIST

For the waveguides described in this thesis, simplicity of fabrication is also desired and can be achieved by incorporating a cross-linking moiety in the material which can be later used to reduce the number of processing steps. This eliminates the requirement of a photoresist layer, as described in Section 1.1.3, as the optical polymer itself is designed to function as a negative photoresist. Typically, a photoresist is a layer coated and patterned on top of the material to be patterned. A photoresist is considered "positive" if the portion exposed to light becomes soluble to developer and "negative" if it be comes i nsoluble so that the rest of the resist material is washed away by developer. The vinyl groups at the *para*-positions of the arene units of both the buffer and guiding materials in this thesis (Figure 2.1) are activated by radical reactions which induce crosslinking, increasing the molecular weight of the polymers and altering their solubility, optical, thermal and mechanical properties.¹

2.1.2 SYNTHETIC CONTROL

The ratio of monomers in each type of polymer influences its refractive index, optical and material properties, and must be controlled for reproducibility of waveguide properties. Variations in polymer composition from each iterative round of synthesis were monitored by G el P ermeation C hromatography and F ourier T ransform I R spectroscopy.

Control over molecular weight and the amount of cross-linking in the guiding material are critical to the success of its behavior as a negative photoresist and the resulting optical devices. If the polymer chains are too large, the features resulting from the material may be poorly defined, meaning the waveguides will have irregular structures resulting in high loss. Furthermore, polymer of too high a molecular weight will not dissolve well in solvents as required for their application to substrate surfaces by spin-coating or organic solvent wet-etching.

Too low a molecular weight would require a much higher degree of cross-linking in or der to behave properly as a negative resist. This could also create i rregular structures as the less stable waveguide walls will be more prone to roughening by the etching process. Also, if the polymer chains are too short the film will be brittle and fragile making it undesirable for contact mask phot olithography. The spin-coating technique and results used in this thesis are described in the next chapter.

2.1.3 POLYMER COMPOSITION

The gui ding pol ymer is comprised of a mixture of styrene (St) and pentafluorostyrene (PFS) monomer units with 4-hydroxystyrene (4HS) added as the cross-linking moiety. This group is attached by replacement of the *para*-positioned fluorine atom on some of the PFS units and the hydrogen of the 4HS hydroxyl group, creating an either bridge. This reaction would not be expected to occur at the ortho-position owing to steric hindrance and substitution exclusive to the *para*-position has been previously observed.²

The buffer polymer is comprised of 4-fluorostyrene (4FS) and PFS with 4HS again added as the cross-linking moiety. The substitution of a fluorinated styrene for standard styrene s erves t o lower t he r efractive index of t he bu ffer l ayer, satisfying the requirements of a waveguide. The incorporation of heavier atoms gives a lower optical dielectric constant, re sulting in a lower r efractive inde x. The c ladding pol ymer designed for these investigations is a mixture of St, PFS, and glycidyl methacrylate (GMA), which was incorporated be cause it c ontains an epoxide, which is a latent

crosslinking moiety, and produces a lower Young's modulus compared with the styrene moieties alone. Mechanically, the "softer" cladding will exert less pressure when it is cured around the ridge waveguide. In this manner, stress-induced birefringence and loss in the guiding core can be reduced. Moreover, the final structure is less susceptible to swelling during feature development.⁴

Due to differences in monomer reactivity ratios, the ratio of monomers in the prepared optical polymers differs from the starting ratio of monomers the reaction mixture. Different monomer units will exhibit different selectivity for free radical polymerization. For some monomer "A" in the copolymerization of "A" with monomer "B", the reactivity ratio, r_A , can be calculated according to Equation 2.1. Here, k_{AA} is the reaction rate constant for "A" adding to another "A" unit and k_{AB} is the reaction rate constant for "A" adding to a unit of "B".

$$r_{A} = \frac{k_{AA}}{k_{AB}} {(2.1)}^{5}$$

A reactivity ratio less than one for a monomer species indicates that it will most probably add to different monomer units and not to its own kind. A ratio greater than one indicates the opposite preference. A reactivity ratio of 1 indicates no preference. Thus, in a mixture of GMA and PFS, the PFS radical in solution has a reactivity ratio of 0.39, indicating that PFS exhibits a much higher preference for GMA than for its own type. The GMA radical exhibits little preference.⁴

Structures of the five primary polymers are presented below in Figure 2.1. The nature of this project required frequents ynthesis of the sematerials, so a naming convention was established to differentiate batches of the same polymer. As presented in Figure 2.1, "cop1" and "cop2" are the precursor copolymers used to make the guiding and buffer polymers, respectively. The guiding polymer is a terpolymer, containing three different monomer units, and is denoted by "ter". The buffer and cladding polymers are also terpolymers, and are denoted "buf" and "clad" for easy reference. With these conventions, "T" stands for trial and "xx" is a variable for the

batch number. F or e xample, *cop1T04* is the 4 th batch pr epared of poly(styrene-co-pentafluorostyrene). S imilarly, batches of 4H S are distinguished as *paraTxx*.

FIGURE 2.1 (a) styrene-co-pentafluorostyrene (cop1Txx); (b) 4-fluorostyrene-co-pentafluorostyrene (cop2Txx); (c) styrene-co-pentafluorostyrene-co-[4-styren-4'-yl-2,3,5,6-tetrafluorophenylether] (terTxx); (d) 4-fluorostyrene-co-pentafluorostyrene-co-[4-styren-4'-yl-2,3,5,6-tetrafluorophenylether] (bufTxx); (e) glycidyl methacrylate-co-styrene-co-pentafluorostyrene (cladTxx).

2.2 EXPERIMENTAL

2.2.1 GENERAL METHODS

All reactions were carried out under an atmosphere of dry argon using standard Schlenk techniques. Polymer syntheses were performed in three-neck, round-bottom flasks ranging in size from 500 mL to 3 L, dependent on scale, with appropriately sized oval-shaped Teflon stirring bars. Each apparatus was fitted with a thermometer in a rubber septum, a glass condenser with argon inlet, and a 24/40 ground glass stopper for reagent and solvent addition and submerged in an oil bath placed on a stirring hotplate. The entire set up was covered with large sheets of foil to minimize light exposure.

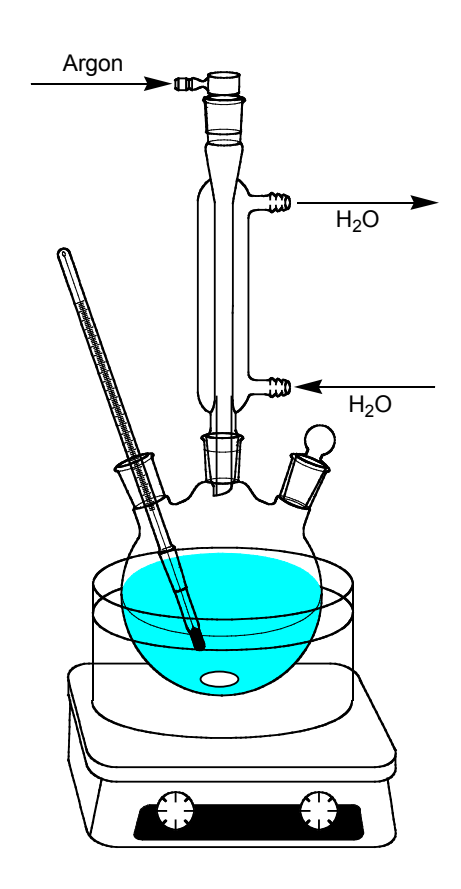


FIGURE 2.2 Typical apparatus for the polymer syntheses described in this chapter.

Pentafluorostyrene, 4-fluorostyrene, styrene and glycidyl methacrylate monomers were pa ssed t hrough pre-packed *tert*-butylcatechol inh ibitor r emover c olumns (*Sigma-Aldrich*) immediately prior to synthesis. *N,N*-Dimethylacetamide was stored under argon over molecular sieves in the original container.

2.2.2 REAGENTS AND MATERIALS

Styrene monomer, 99%, was obtained from Aldrich. Pentafluorostyrene (PFS) and 4-fluorostyrene (4FS) were obtained from SynQuest Laboratories. 4-acetoxystyrene, *N*,*N*-Dimethylacetamide (DMA), 99.8%, and propyl a cetate, 99.5%, were obtained from Sigma-Aldrich. Benzoyl peroxide (BPO), 97%, and sodium hydride (NaH), 95%, were obtained from Aldrich. Chloroform was acquired from ACP Chemicals. Hexanes, methanol, and toluene were acquired from EMD Chemicals. Toluene was distilled over calcium hydride (CaH) under nitrogen immediately prior to use. CaH, Sodium chloride (NaCl), potassium hydroxide (KOH), activated charcoal (Norit-A decolorizing carbon), and magnesium sulfate (MgSO₄) were acquired from Fisher. Concentrated acetic acid, ≥99.7%, and n-pentane were also acquired from Fisher. Milli-Q® water was collected from a Milli-Q® Ultrapure Water Purification System. Glycidyl methacrylate (GMA), ≥97.0%, and Celite 545 or 500, fine grade, were acquired from Fluka.

2.2.3 PREPARATION OF MATERIALS FOR POLYMER SYNTHESIS

2.2.3.1 Purification of Benzoyl Peroxide (BPO)

15.0 g (0.0619 mol) BPO was dissolved in 250 mL. Additional chloroform was added if complete dissolution was not achieved with the initial volume. An equivalent volume of methanol was added in approximately 2 m L portions using a disposable pipette to i nduce precipitation. Upt o 100 mL additional methanol was added if precipitation did not appear complete. The purified product was collected and dried for three hours on a fritted glass filter under vacuum. Purified BPO appeared as a fine, white, crystalline powder in about 80% yield and refrigerated for a period of up to 6

months dependent on laboratory humidity. (USE EXTREME CAUTION: MATERIAL IS EXPLOSIVE, AUTOIGNITION TEMPERATURE OF 80°C)

2.2.3.2 Synthesis of 4-hydroxystyrene (4HS or *paraTxx*)

A concentrated solution of KOH (84 g, 1.5 mol) in Milli-Q® water (100 mL) was prepared a day in advance and stored in the refrigerator. NaCl was used to prepare an ice bath with temperature between -5 and 0 °C. Approximately 100g NaCl was required per 1 L of water and ice. The reaction vessel was a 2 L, three-neck, round-bottom flask fitted with a thermometer in a rubber septum, 250 mL dropping funnel with argon inlet, and a 24/40 ground glass stopper for reagent and solvent addition and submerged in the ice bath placed on a stir plate. The vessel was flushed with argon and 720 mL Milli-Q® H_2O and 80 g (0.49 mol) 4-acetoxystyrene were added. The two liquids are insoluble so vigorous stirring w as r equired. The c hilled K OH s olution was t ransferred to the dropping funnel and added dropwise. The set up was covered with foil to minimize light exposure and the reaction was allowed to proceed between 0 and 5 °C for three hours.

The resulting clear, yellow solution was acidified to promote product precipitation with 120 mL of a 1:1 by volume solution of Milli-Q® water and glacial acetic acid. The thick, white sludge of the product mixture was tested to determine that a pH of at least 6 had been attained. If not, more of the water-acid mixture was added until pH 6 was achieved. The solid product was separated and dried by vacuum filtration on a large Buchner funnel with 125 mm filter paper and left to dry under light vacuum, covered with foil to reduce contamination, overnight.

4-hydroxystyrene was recrystallized from approximately 20 times its mass of an 80:20 hexanes:pentane solution. For example, 40 g of impure product required 800 mL of solution for purification. The product and solvents were combined and he ated to 45-50 °C to dissolve the solid. Upon complete dissolution, 2.3 g activated charcoal was added and stirred for five minutes. Any water remaining in the system was removed by the a dsorption w ith a pproximately 40 g M gSO₄. The solution w as h ot f iltered t o remove the charcoal and drying agent. This flask was sealed and refrigerated for 48

hours to precipitate the purified 4-hydroxystyrene. The product was collected via vacuum filtration on a large Buchner funnel and rinsed with pentane. This shiny, flaky, white product was left to dry under vacuum for a pproximately three hours be fore transfer to a Nalgene® bottle sealed with Parafilm® and covered with aluminum foil to prevent light exposure. The product was then stored in the refrigerator.

2.2.4 POLYMER SYNTHESIS

2.2.4.1 Synthesis of Guiding Polymer P recursor, S tyrene-co-pentafluorostyrene (cop1Txx)

100.0 mL (0.3664 mol) pentafluorostyrene, 20.8 mL (0.220 mol) styrene and 400 mL toluene were combined and stirred for 5 min. 1.54 g (0.00636 mol) BPO and 200 mL toluene were added and stirred for 5 min. The set up w as covered with foil to minimize light exposure and the mixture was heated to 80 °C over 1 h and allowed to react at this temperature for 20 h. The reaction mixture was subsequently cooled to room temperature with stirring and argon atmosphere maintained.

The polymeric product was separated from the excess of the reaction mixture by precipitation in acidified methanol. Accordingly, the mixture was transferred to a dropping funnel and added drop-wise into 10 times its volume of methanol plus 0.5% by volume of acetic acid. The precipitate was collected on a 4 L capacity tabletop Buchner funnel with 2 4.0 cm diameter Whatman #1 f ilter pa per un der maximum in-house vacuum. The solid product was left to dry on the funnel under light vacuum, covered with foil to reduce contamination, overnight.

The collected solid was dissolved in approximately 400 mL distilled toluene. This solution was filtered under vacuum through approximately 1 cm of Celite sandwiched between two pieces of 125 mm diameter Whatman #1 filter paper on a Buchner funnel into a 1 L filtering flask. The filtered solution was precipitated by drop-wise addition to 10 times its volume of methanol and collected on a 4 L capacity tabletop Buchner funnel with 24.0 cm diameter Whatman #1 filter paper under maximum house vacuum. The solid product was left to dry on the funnel under light vacuum, covered with

aluminum foil to reduce contamination, overnight. This purification was performed at least twice. The final purified product was stored in a Nalgene bottle sealed with Parafilm and characterized.

2.2.4.2 Synthesis of Guiding Polymer, Styrene-*co*-pentafluorostyrene-*co*-[4-styren-4'-yl-2,3,5,6-tetrafluorophenylether] (*terTxx*)

40.0 g *cop1Txx* and 5.62 g (0.468 mol) 4-hydroxystyrene were combined. The bottle c ontaining *N*,*N*-dimethylacetamide (DMA) was f lushed w ith a rgon. 300 m L DMA were added to the reaction vessel in multiple portions using a 50 mL glass syringe and 12 inch, small gauge syringe needle. 1.28 g (0.0533 mol) NaH was added to the reaction mixture in two portions f or s afer handling *(USE EXTREME CAUTION: MOISTURE REAC TIVE M ATERIAL)*. I mmediately f ollowing t he a ddition of e ach portion, 50 mL DMA was added in such a manner as to rinse NaH from the sides of the interior of the flask, bringing the total volume of DMA to 400 mL. Addition of NaH caused the reaction mixture to change from clear and colorless to frothy pink, and then to a clear, deep reddish brown.

The mixture was stirred for 30 min then gradually heated to 106 °C over the course of a n hour. This temperature was maintained for two hours. The mixture was then cooled below 30 °C before product recovery.

The polymeric product was separated from the excess of the reaction mixture via precipitation. Separation and purification of *terTxx* is identical to that of *cop1Txx*, described previously in Section 2.2.4.1. Additional toluene was used as precipitation solvent if necessary. The final purified product was stored in a Nalgene bottle sealed with Parafilm, covered with aluminum foil to prevent light exposure and characterized by DSC, TGA, NMR, and ATR FT-IR.

2.2.4.3 S ynthesis of B uffer P olymer P recursor, 4 -fluorostyrene-copentafluorostyrene (cop2Txx)

100.0 mL (0.3664 mol) pentafluorostyrene, 21.6 mL (0.173 mol) 4-fluorostyrene and 400 mL propyl acetate combined and stirred for 5 min. 1.54 g (0.00636 mol) BPO and 200 mL propyl acetate were added and stirred for 5 min. The set up was covered

with foil to minimize light exposure and the mixture was heated to 80 °C over one hour and allowed to react at t his temperature f or 20 h. The r eaction mixture w as subsequently c ooled t o r oom t emperature with s tirring a nd a rgon a tmosphere maintained.

Separation and purification of *cop2Txx* is identical to that of *cop1Txx*, described previously in Section 2.2.4.1.

2.2.4.4 S ynthesis o f B uffer P olymer, 4 -fluorostyrene-co-pentafluorostyrene-co-[4-styren-4'-yl-2,3,5,6-tetrafluorophenylether] (bufTxx)

The manner of preparing *bufTxx* is highly similar to that of the guiding polymer, *terTxx*, described in Section 2.2.4.2 above. The major point off differentiation is the starting material. The copolymer to be functionalized with 4-hydroxystyrene in the buffer polymer synthesis is *cop2Txx* instead of *cop1Txx*. 40.0 g of *cop2Txx* and 5.62 g (0.468 mol) 4-hydroxystyrene are used. All other materials, amounts, and techniques are the same are described in 2.2.4.2.

2.2.4.5 Synthesis of Cladding Polymer, Glycidyl methacrylate-*co*-styrene-*co*-pentafluorostyrene (*cladTxx*)

71.1 mL (0.261 mol) pentafluorostyrene, 16.2 mL (0.172 mol) styrene, 50.8 mL glycidyl m ethacrylate (0.334 mol) were combined a nd s tirred f or 5 min. 1.95 g (0.00805 mol) BPO and 330 mL toluene were added and stirred for 5 min. The set up was covered in foil to minimize light exposure and the mixture was heated to 70 °C over 1 h and allowed to react at this temperature for 20 h. The reaction mixture was very viscous at this point. An additional 330 mL toluene was added in approximately 50 mL portions to reduce viscocity as the mixture cooled to room temperature with stirring maintained.

The polymeric product was separated from the excess of the reaction mixture via precipitation. The mixture was transferred to a dropping funnel and added drop-wise into 10 t imes i ts vo lume of methanol pl us 0 .5% by vol ume of a cetic a cid. The precipitate formed was collected on a 4 L capacity tabletop Buchner funnel with 24.0 cm diameter Whatman #1 filter paper under maximum in-house vacuum. The solid

product was left to dry on the funnel under light vacuum, covered with foil to reduce contamination, overnight.

The collected solid was dissolved in a minimum of distilled toluene. This solution was filtered under vacuum through approximately 1 cm of Celite sandwiched between two pieces of 125 mm diameter Whatman #1 filter paper on a Buchner funnel into a 1 L filtering flask. The filtered solution was precipitated by drop-wise addition to 10 times its volume of methanol and collected on a 4 L capacity tabletop Buchner funnel with 24.0 cm diameter Whatman #1 filter paper under maximum house vacuum. The solid product was left to dry on the funnel under light vacuum, covered with aluminum foil to reduce contamination, overnight.

2.3 RESULTS AND DISCUSSION

One of the objectives of this thesis was to demonstrate that polymer films for integrated optics can be prepared with reproducible optical properties, particularly the refractive index. Therefore, it is important to demonstrate that the properties of the polymers giving rise to a given refractive index are well controlled. These properties are controlled by managing the relative ratio of comonomers in the final composition, which in turn can be determined by infrared spectroscopy. Final confirmation concerning reproducibility of the waveguide devices in the following chapter was based on refractive index measurements. All polymers and precursors were reproducibly prepared as judged by infrared, with the exception of *cladTxx*. The following a nalyses of reproducibility and physical properties performed on the polymers confirmed their suitability for the fabrication of waveguides by lithography.

The first batch of cladding which was prepared, *cladT01*, resulted in a gummy, solvent-logged mass which hardened into a glassy solid as the solvent evaporated over two days. This is likely due to the molecular weigh and chain length being higher than desired. The reaction time was preformed on 1/4 th scale for *cladT02*, and the

precipitation procedure was a djusted sot hat additional solvent was a dded prior to precipitation and before the reaction mixture cooled (as described in the Experimental section above). This produced the desired powdered form of the product which was purified on ce. Unfortunately this batch was found to be unusable owing to its insolubility in the spin-coating solvent.

2.3.1 A TTENUATED T OTAL REF LECTION F OURIER TRAN SFORM INFRARED (ATR FT-IR) SPECTROSCOPY

IR spectra were collected using a PerkinElmer Spectrum BX spectrometer. Data were automatically baseline corrected to account for the attenuated total reflection and background by analysis software, *Spectrum*.

ATR FT-IR is a contact sampling method where the sample is pressed directly to the diamond infrared crystal. The spectra commonly exhibit small shifts in frequency (<20 cm⁻¹) and differences in peak intensity when compared to transmission FT-IR spectra.⁶ A lower percent transmittance, %T, in an ATR spectrum indicates a stronger band whereas high %T values correspond to strong bands in transmittance FT-IR.

2.3.1.1 Characterization of Polymers and Precursors

One representative spectrum of each material investigated is presented in Figures 2.3-7. An I R s pectrum of the monomer 4-hydroxystyrene (4HS) was collected to confirm that replacement of the acetoxyl group of 4-acetoxystyrene by hydroxyl group was successful in each batch. In Figure 2.3 the broad band near 3400 cm⁻¹ indicates the presence of the hydroxyl group.

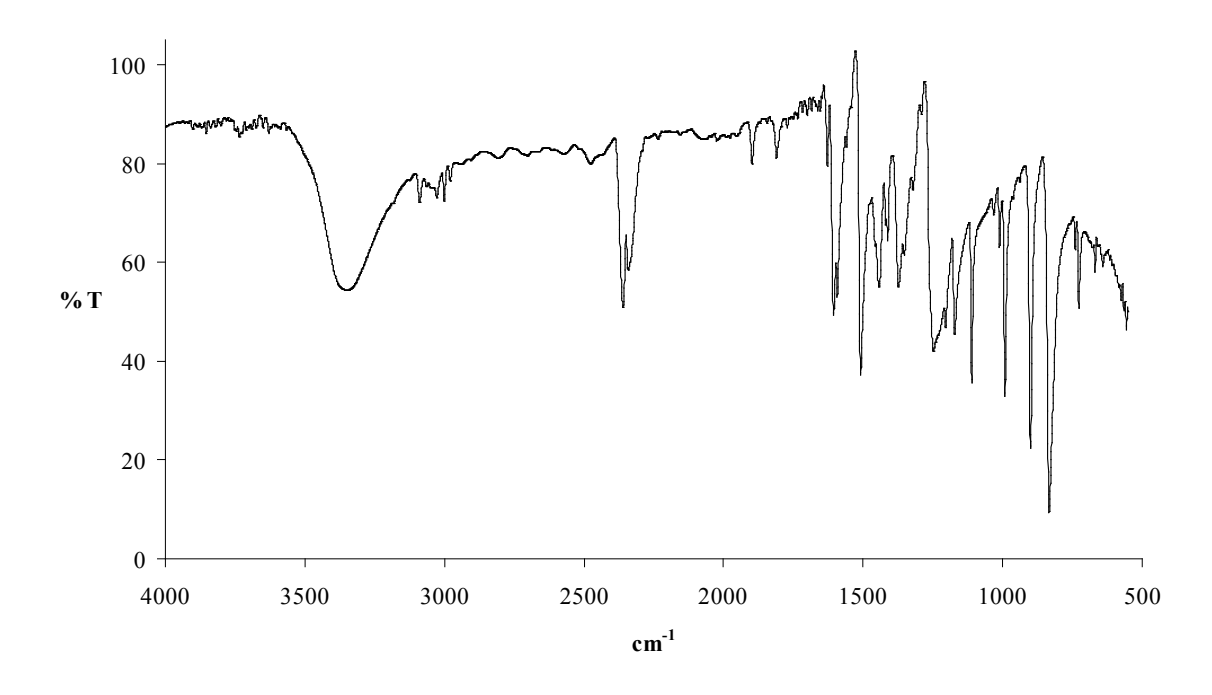


FIGURE 2.3 FT-IR Spectrum of paraT06 (4HS) (Not baseline corrected)

In the polymers, specific peaks confirmed the presence of different monomer units. These characteristic peaks are listed in Table 2.1. The single peak found around 1652 cm⁻¹ in the spectra of all four polymers, *cop1Txx*, *terTxx*, *cop2Txx*, and *bufTxx*, is assigned to an overtone of the C=C stretching of the pentafluorosubstituted aromatic ring of pentafluorostyrene (PFS). This peak is present in the transmission FT-IR spectrum of 2,3,4,5,6 -pentafluorostyrene and a bsent from spectra of the other monomers. The shoulder observed on the lower energy side of this peak in *cop1Txx* and *cop2Txx* evolves into a weak peak at 1635 cm⁻¹ in *terTxx* and *bufTxx* and results from C=C stretching of the vinyl group attached to the crosslinking group added by functionalization. This group is from 4HS, the cross-linking moiety, which is added by the formation of an ether bridge at the *para* position of the fluorinated ring of PFS. Functionalization is also confirmed by the presence of a C-O-C stretching vibration at 1210 cm⁻¹ in *terTxx* and *bufTxx*.

The C-H vibration of the *H*-styrene moiety was observed at approximately 702 cm⁻¹ in both cop1Txx and terTxx. The band at 1606 cm⁻¹ in cop2Txx and 1604 cm⁻¹ in

bufTxx is a ttributed to 4-fluorostyrene (4FS) since it is present in the transmission FT-IR spe ctrum of the monomer molecule and absent from spe ctra of the other monomers.⁸

TABLE 2.1 Characteristic FT-IR Peaks of the Optical Polymers

POLYMER	C=C	=C-F	С-О-С	=С-Н
	(cm ⁻¹)	(cm ⁻¹)	(cm ⁻¹)	(cm ⁻¹)
cop1	1652.5			701.5
ter	1652		1210.4	701.5
cop2	1652.5	1606.2		
buf	1652	1604	1210.6	

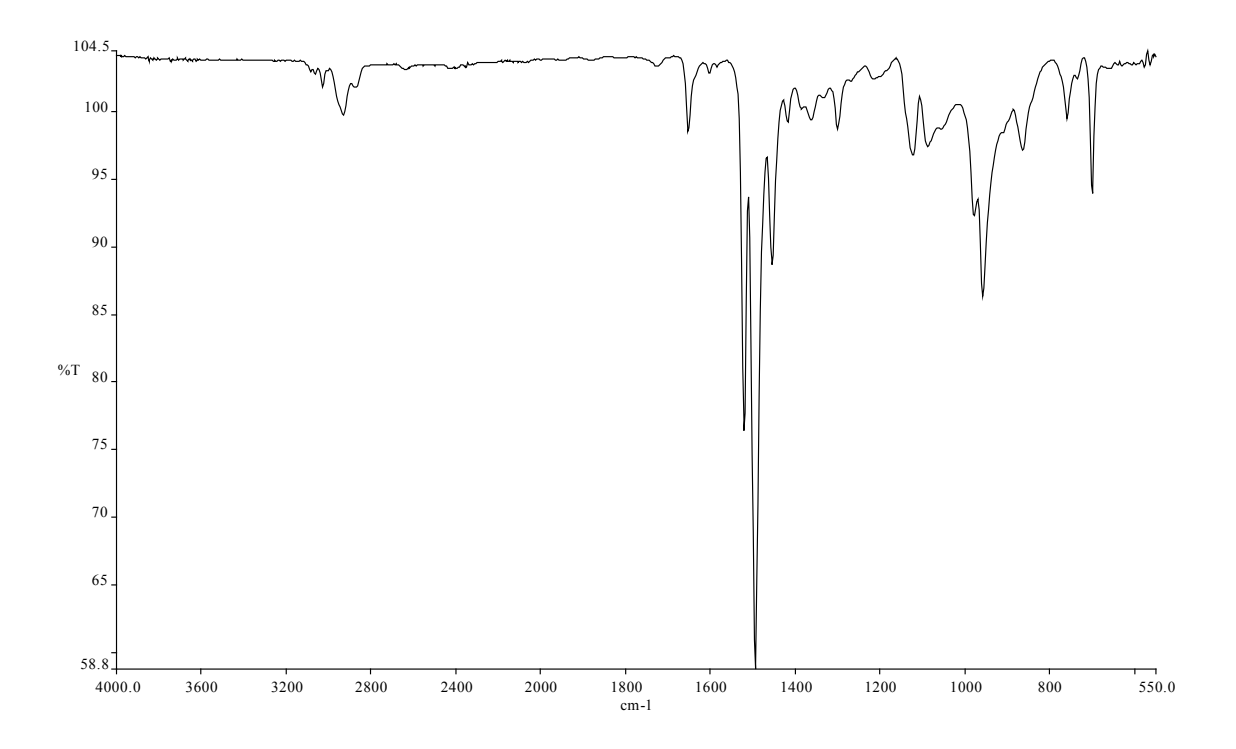


FIGURE 2.4 FT-IR Spectrum of cop1T11

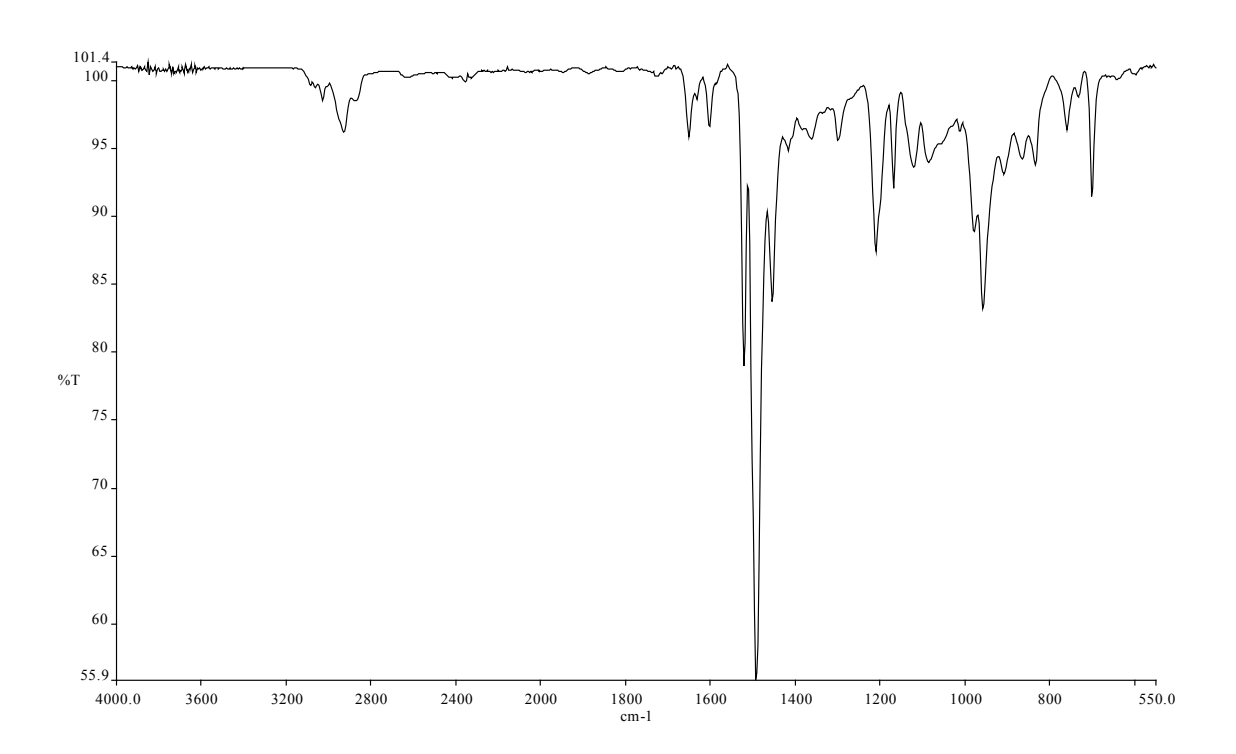


FIGURE 2.5 FT-IR Spectrum of *terT20*

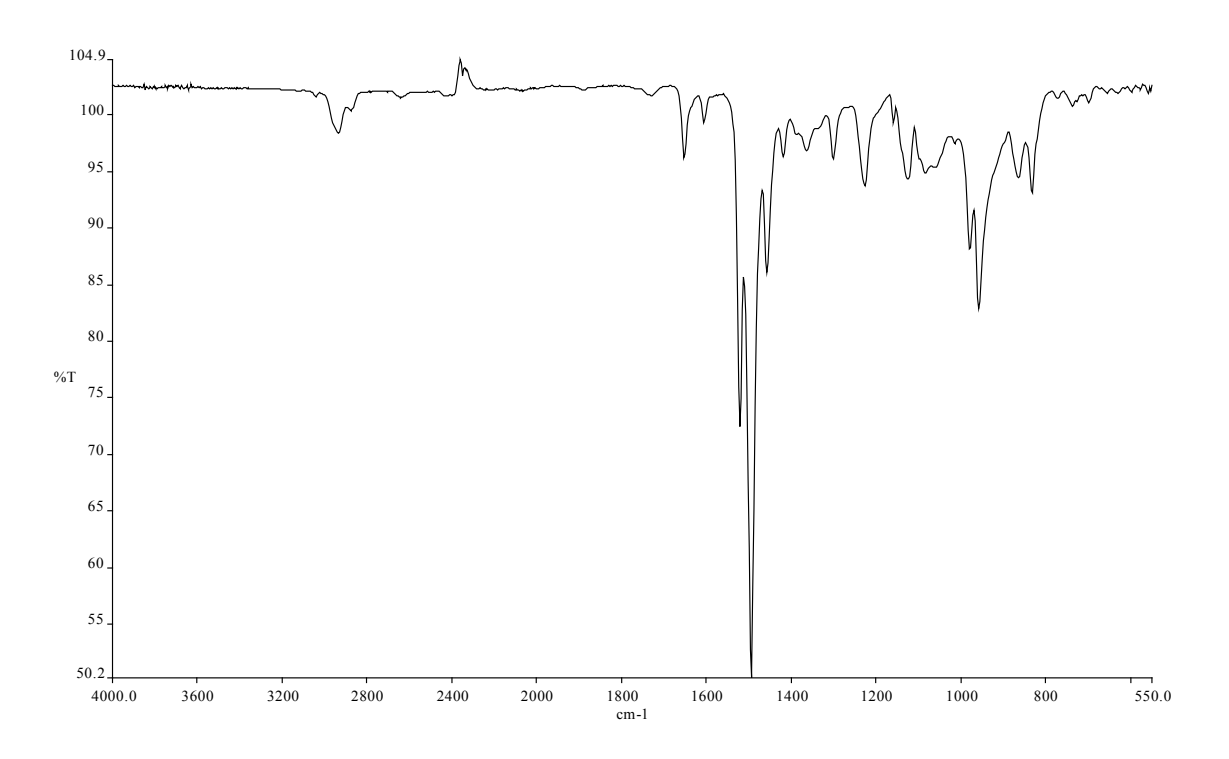


FIGURE 2.6 FT-IR Spectrum of *cop2T02*

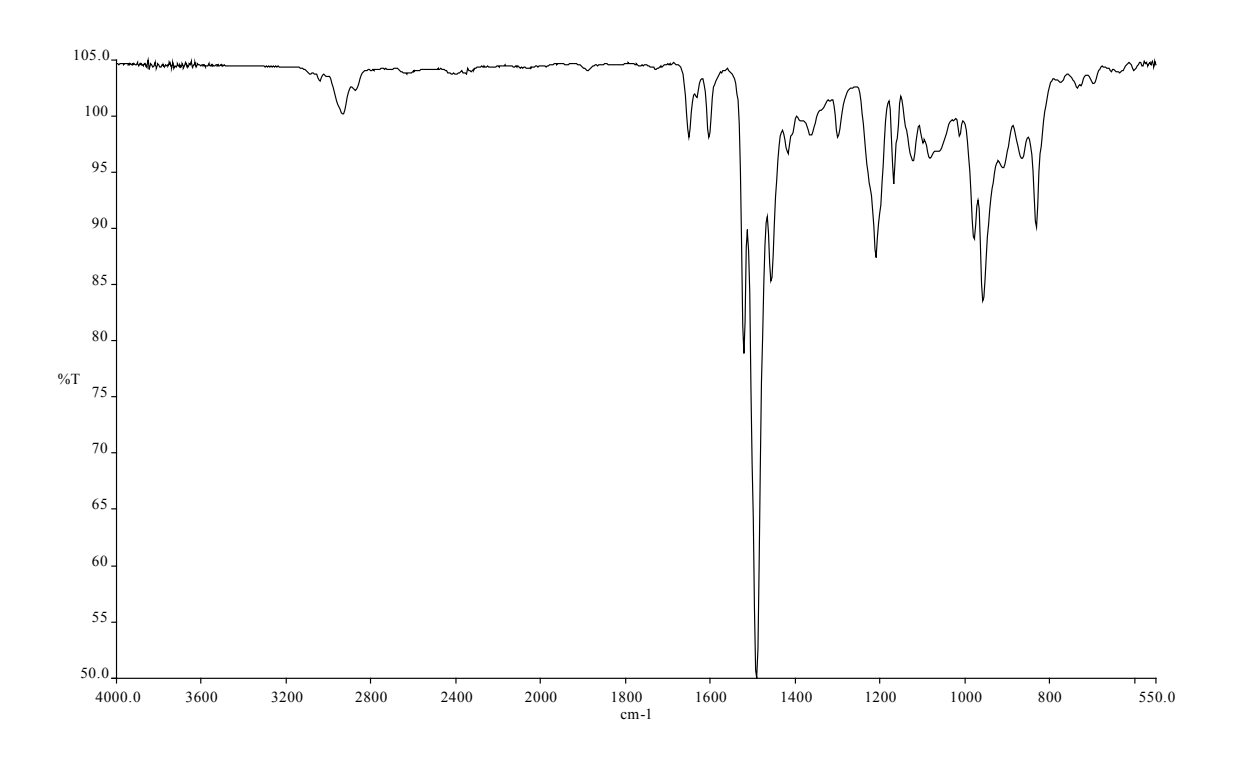


FIGURE 2.7 FT-IR Spectrum of bufT06

2.3.1.2 Analysis of Reproducibility

Multiple batches of the polymers were analyzed to determine reproducibility. For all four polymer compositions, comparison of the different batches shows that all are highly similar with respect to the presence of all peaks, both weak and strong, as well as relative transmittance.

As noted above, the monomer ratio must be controlled because each monomer contributes differently to the index of refraction. Here, we show the results of a quantitative analysis of polymers *terTxx* and *bufTxx*. We monitored the ratios of =C-H or =C-F to C=C peaks and C-O-C to C=C peaks for each batch and compared them. The results are presented in Table 2.2. An analysis of the peak ratios of different batches of the same material reveals good batch-to-batch reproducibility.

TABLE 2.2 Reproducibility of Guiding and Buffer Polymer Syntheses by Comparison of FT-IR Peak Ratios. (* *bufT03* is not included in the average and standard deviation calculations because it was determined to be unacceptable for lithographic experimentation.)

GUIDE	(=C-H)	(C-O-C)
BATCH	to (C=C)	to (C=C)
terT17	1.84	2.59
terT19	1.78	2.60
terT20	1.80	2.55
terT21	1.70	2.39
terT22	1.68	2.34
terT23	1.82	2.66
AVERAGE	1.77	2.52
STD. DEV.	0.067	0.128

BUFFER	(=C-F)	(C-O-C)
BATCH	to (C=C)	to (C=C)
bufT03*	0.92	1.93
bufT04	1.02	2.73
bufT05	0.98	2.52
bufT06	0.99	2.54
AVERAGE*	1.00	2.60
STD. DEV.*	0.019	0.114

2.3.2 GEL PERMEATION CHROMATOGRAPHY (GPC)

Gel permeation chromatography (GPC), a type of size exclusion chromatography, was used to obtain molecular weight a verages and polydispersities of the polymers. GPC was performed with a Waters 510 liquid chromatography pump equipped with two Styragel columns (HR1 and HR4) connected in series. Measurements were taken at room temperature in tetrahydrofuran. Polystyrene standards from Scientific Polymer Products, Inc. were used to calibrate the columns under the same conditions to be used for the polymer samples.

Typically, t he r etention vol ume s cale r ecorded i s t ransposed t o the va rying molecular weight sca les us ing correct ca libration curves. Because st yrene homo polymer standards were used, the instrument is calibrated only approximately with respect to the fluorinated polymer samples. Back-to-back c hromatograms t aken of *cop1T12* gave weight average molecular weights which differed by 2000 D. The values presented in Table 2.3 corresponding to *cop1T12* are the averages of those two runs.

The number a verage, M_n , and weight a verage, M_w , molecular weights and the polydispersity index, PDI, are presented in the summary of results found in Table 2.3 They are defined below as Equations 2.2-4. The molecular weight of cop1Txx is lower than that of cop2Txx. Styrene monomer units constitute a similar fraction of cop1Txx as the heavier 4-fluorostyrene (4FS) monomer units do of cop2Txx according to NMR analysis described in Section 2.3.3.2. Similarly, terTxx exhibits a lower MW value than bufTxx.

$$M_{w} = \frac{\sum_{i} N_{i} M_{i}^{2}}{\sum_{i} N_{i} M_{i}}$$
 (2.2)

$$M_n = \frac{\sum_i N_i M_i}{\sum_i N_i}$$
 (2.3)

$$PDI = M_w/M_n ag{2.4}$$

 M_w = weight average molecular weight

 M_n = number average molecular weight

i = number of unique molecular weights

 N_i = number of molecules with molecular weight M_i

M =molecular weight

PDI = polydispersity index

The polydispersities of a ll the polymers are low. A typical average range for polymers produced by radical initiation is 1.8-3.¹⁰ Low polydispersity in our samples is desirable a sit indicates a more narrow distribution of chain lengths. Both functionalized terpolymers, *terTxx* and *bufTxx*, exhibit higher MW values and slightly higher polydispersity than their copolymer precursors, *cop1Txx* and *cop2Txx*. This is expected, as their syntheses are primarily functionalizations, adding only mass to the polymer chains.

TABLE 2.3 Summary of GPC Analysis of the Polymers

POLYMER	M _w	M _n		
ВАТСН	(D)	(D)	PDI	
cop1T08	27099	17463	1.55	
cop1T09	26685	16378	1.63	
cop1T10	24885	15868	1.57	
cop1T12	30669	18976	1.62	
cop1T13	29732	18514	1.61	
AVERAGE	27814	17440	1.59	
STD. DEV.	2356	1333	0.033	
terT17	40206	24691	1.63	
terT20	42732	25200	1.70	
terT21	47038	26870	1.75	
terT22	40721	23065	1.77	
terT23	45215	26634	1.70	
AVERAGE	43182	25292	1.71	
STD. DEV.	2921	1551	0.054	
cop2T02	47254	28120	1.68	
bufT04	69866	37361	1.87	
bufT05	71270	38873	1.83	
bufT06	62050	34085	1.82	
AVERAGE	67728	36773	1.84	
STD. DEV.	4968	2448	0.026	

2.3.3 ¹H NUCLEAR MAGNETIC RESONANCE (NMR) SPECTROSCOPY

Proton NMR spectra were taken of the polymers in deuterated dichloromethane (CD_2Cl_2) at 400 or 500 MHz to determine the ratio of monomers in each material. Measurements were conducted with a 5 s relaxation delay.

All polymers examined gave spectra with a group of broad peaks in the alkyl region between 1.2-3 ppm resulting from the three protons of each monomer unit along the polymer backbone. The functionalized polymers, *terTxx* and *bufTxx*, also exhibited a pair of peaks due to the three vinyl protons of 4-hydroxystyrene at 5.2 and 5.7 ppm. All polymers also gave a group of peaks in the aromatic region between 6.4-7.5 ppm. For *cop1Txx* this was from the five hydrogens on each styrene unit, while for *cop2Txx* it

was from the four hydrogens on each 4-fluorostyrene unit. For terTxx the aromatic peaks were a combination of styrene and 4-hydroxystyrene signals. Similarly, for bufTxx the aromatic peaks are a combination of 4-fluorostyrene and 4-hydroxystyrene signals. The r esults are presented in Table 2.4 and summarized in Table 2.5. Representative spectra of *cop2Txx* and *bufTxx* are presented in Figures 2.8-9.

The guiding polymer composition by number of monomer units, not weight, was determined to be approximately 30.7 %, 53.7 % unfunctionalized pentafluorostyrene, and 12.0 % pentafluorostyrene containing the crosslinking moiety. The buffer polymer was found to c ontain about 21.1 % para-fluorostyrene, 65.4 % unfunctionalized pentafluorostyrene, and 13.5 % pentafluorostyrene containing the crosslinking moiety.

TABLE 2.4 Summary of ¹H NMR Analysis of the Polymers

POLYMER	MONOMER	POLYMER	MONOMER
BATCH	COMPOSITION	BATCH	COMPOSITION
	STY	•	4HS
cop1T08	30.3%	terT10	11.8%
cop1T10	30.7%	terT13*	8.6%
cop1T12	28.6%	terT17	12.2%
cop1T13	33.0%	AVERAGE:	* 12.0%
AVERAGE	30.7%	STD. DEV.	0.3%
STD. DEV.	1.8%		4HS
_	4FS	bufT04	13.5%
cop2T02	21.1%		

TABLE 2.5 Polymer Composition Estimates by ¹H NMR

POLYMER	STY	4FS	PFS	4HS
cop1	30.7%		69.3%	
ter	30.7%		57.3%	12.0%
cop2		21.1%	78.9%	
buf		21.1%	65.4%	13.5%

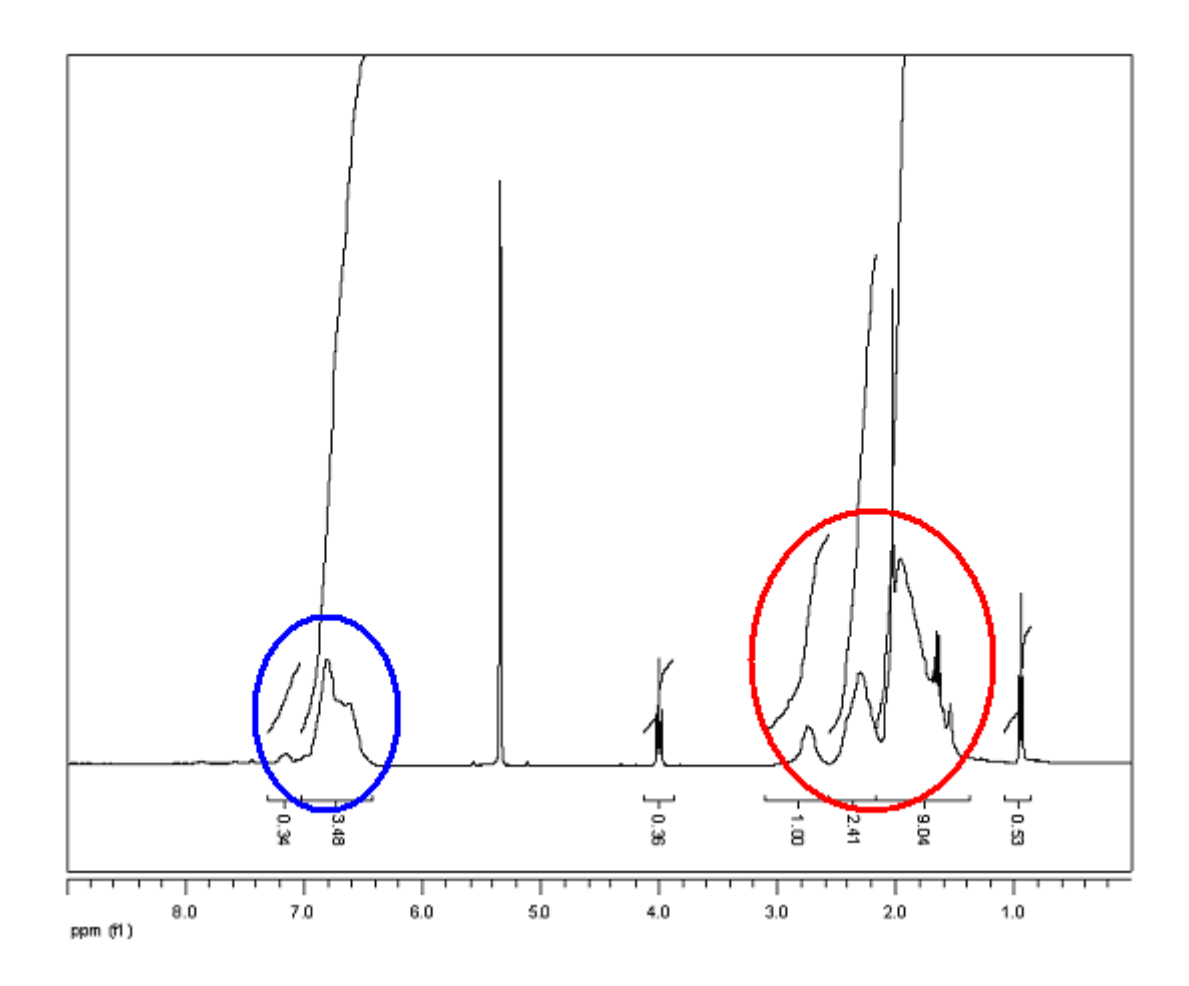


FIGURE 2.8 ¹H NMR Spectrum of *cop2T02* at 400 MHz in CD₂Cl₂. Peaks circled in blue correspond to aromatic p rotons and p eaks circled in red c orrespond to a lkyl protons, as indicated in the polymer structure.

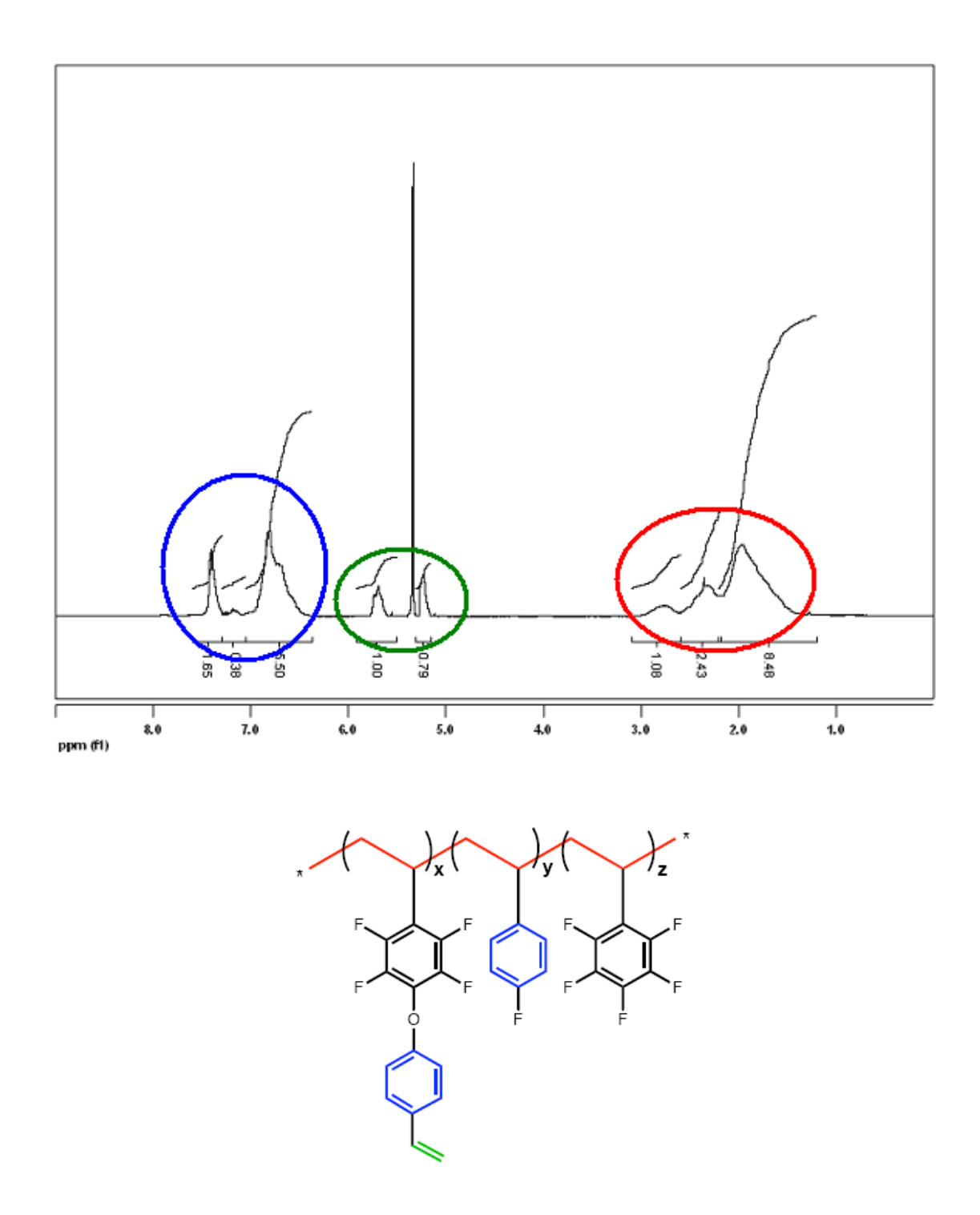


FIGURE 2.9 ¹H NMR Spectrum of *bufT04* at 500 MHz in CD₂Cl₂. Peaks circled in blue correspond to aromatic protons, peaks circled in red correspond to alkyl protons, and peaks circled in green correspond to vinyl protons, as indicated in the polymer structure below:

2.3.4 THERMAL ANALYSIS

Thermal G ravimetric A nalysis (T GA) and Differential S canning Calorimetry (DSC) were used for thermal analysis. Materials for optical devices must be thermo-oxidatively stable at temperatures used for fabrication and device operation. Processing of opto-electronic devices, for example, requires temperatures of 150-200 °C for soldering of one device to another and devices must be able to withstand long term exposure to operational temperatures between -20 and 100 °C. 11

Both the guiding material, terTxx, and the buffer material, bufTxx, show potential in optical device fabrication. They were analyzed here as un-crosslinked pow dered polymers. In device form, these materials would undergo photocuring, increasing their thermal stability above the results presented in this section. The polymer bufTxx was heated above its determined glass transition temperature (T_g) as a way to activate crosslinking and promote curing in a subsequent hard baking steps. The active guiding material, terTxx, was submitted to a hard bake approximately 100 °C above its T_g only after it had been photocured by UV exposure. Both methods are detailed later in Section 3.2.5.1 of this thesis.

2.3.4.1 Thermal Gravimetric Analysis (TGA)

TGA was performed using a TA Instruments Q500 apparatus and analyzed using TA Instruments Universal Analysis 2000 program. Between 4 and 7 mg of sample were used for each run, contained in a hanging platinum crucible. The sample mass can create slight variations in observed decomposition temperature, meaning this method of analysis is not quantitatively precise. All samples were subjected to the same program whereby they were heated from room temperature to 700 °C at a rate of 20 °C/min. The gas used was switched automatically by the instrument from nitrogen to compressed air at 550 °C. Scans of *cop1T12* and *terT19* are presented in Figures 2.10-11.

Copolymers cop1Txx and cop2Txx exhibit single-stage de composition s pectra, indicating that the polymers are of uniform composition. For terTxx and bufTxx the

spectra show ed a clearly resolved, two-stage decomposition with the majority of sample mass lost in the first stage. This is a common phenomenon observed in functional polymers. The first phase of decomposition, thermal depolymerization, removes about three-fourths of the total mass of *terT19*. However, some crosslinking of the functional moieties occurs at the high temperature of the analysis, making a portion of the material more stable and therefore only lost during combustion in the presence of compressed at a bove 5 50 °C. Additionally, the aberration in the second stage of decomposition is the result of the material becoming adhesive and appeared in most analyses of the guiding polymer.

The earliest sign of decomposition in all four polymers was near 400 °C, which is above the r equirements of commercial optical materials. Cured and crosslinked samples of the guiding and buffer materials would likely prove more thermally stable than the un-crosslinked powder samples analyzed here.

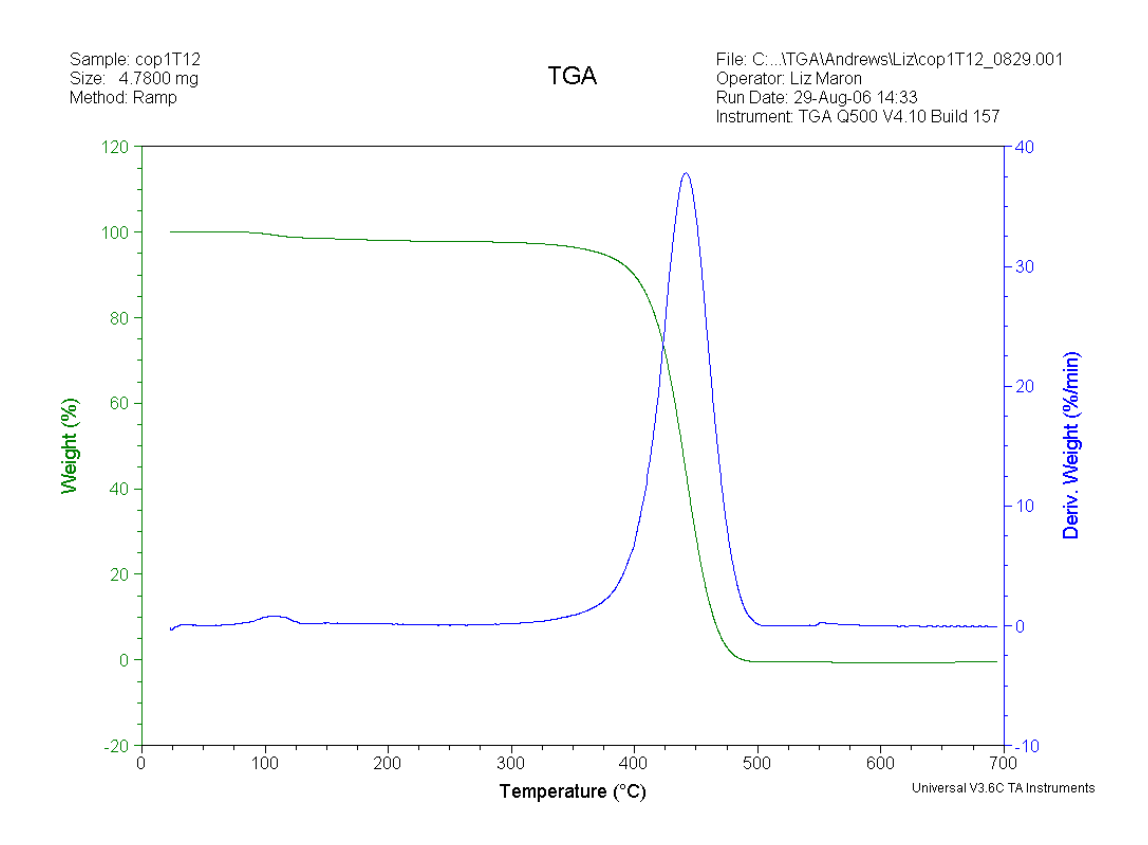


FIGURE 2.10 Thermal Gravimetric Analysis Spectrum of cop1T12

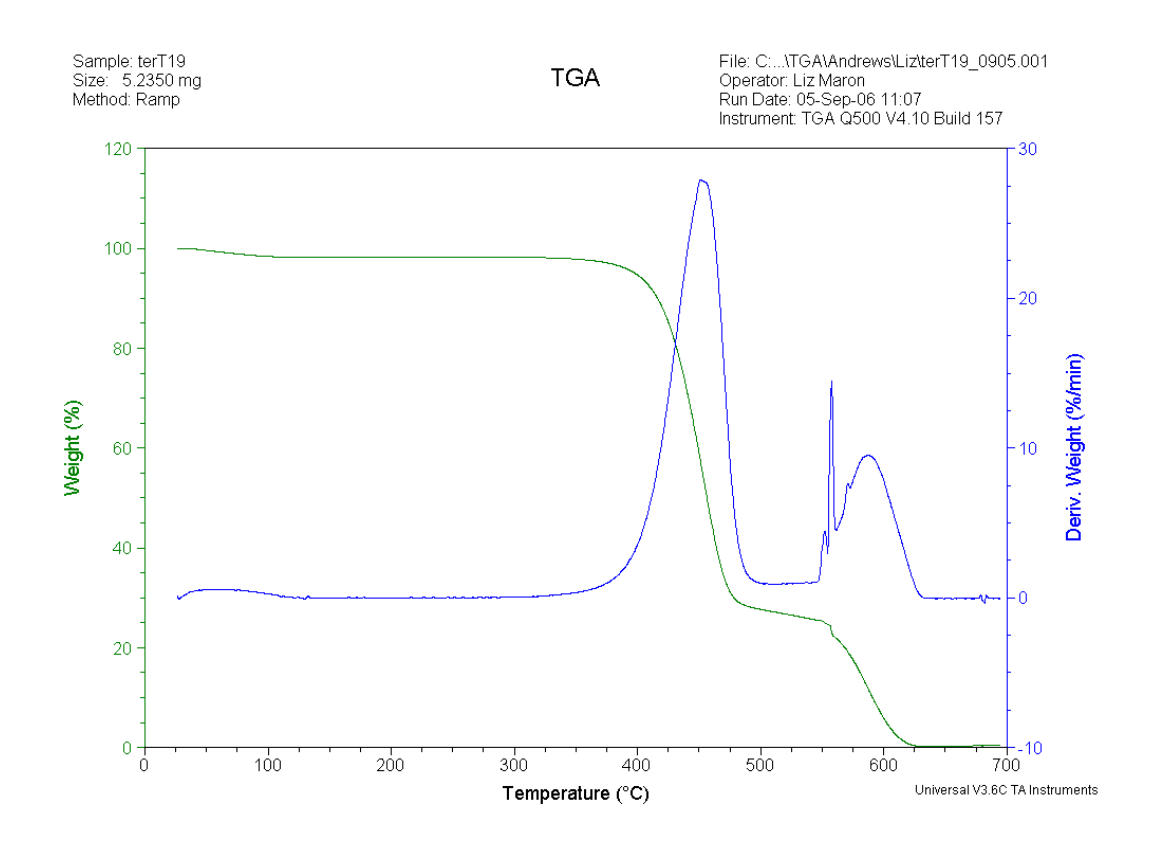


FIGURE 2.11 Thermal Gravimetric Analysis Spectrum of terT19

2.3.4.2 Differential Scanning Calorimetry (DSC)

DSC was performed on a TA Instruments Q1000 apparatus and also analyzed using TA Instruments Universal Analysis 200 program. Between 3 and 7 mg of sample were used for each run, contained in an aluminum pans with new calibrations performed before each set of runs. All samples were subjected to the same "he at-cool-heat" sequence: the scan was started at 50 °C and raised to 150 °C by 10 °C/min then cooled back to 50 °C and raised again to 150 °C at the same rate. The initial heating was necessary to separate any water impurities from the sample such that the curve of the second heating could be used to determine the glass transition temperature, T_g , of each polymer. Scans of *cop1T12* and *terT21* are presented in Figures 2.12-13 and the results are summarized in Table 2.6. The glass transition temperatures of all the polymers are similar to the reported T_g of polystyrene, 100 °C, and pentafluorostyrene, 105 °C. 12

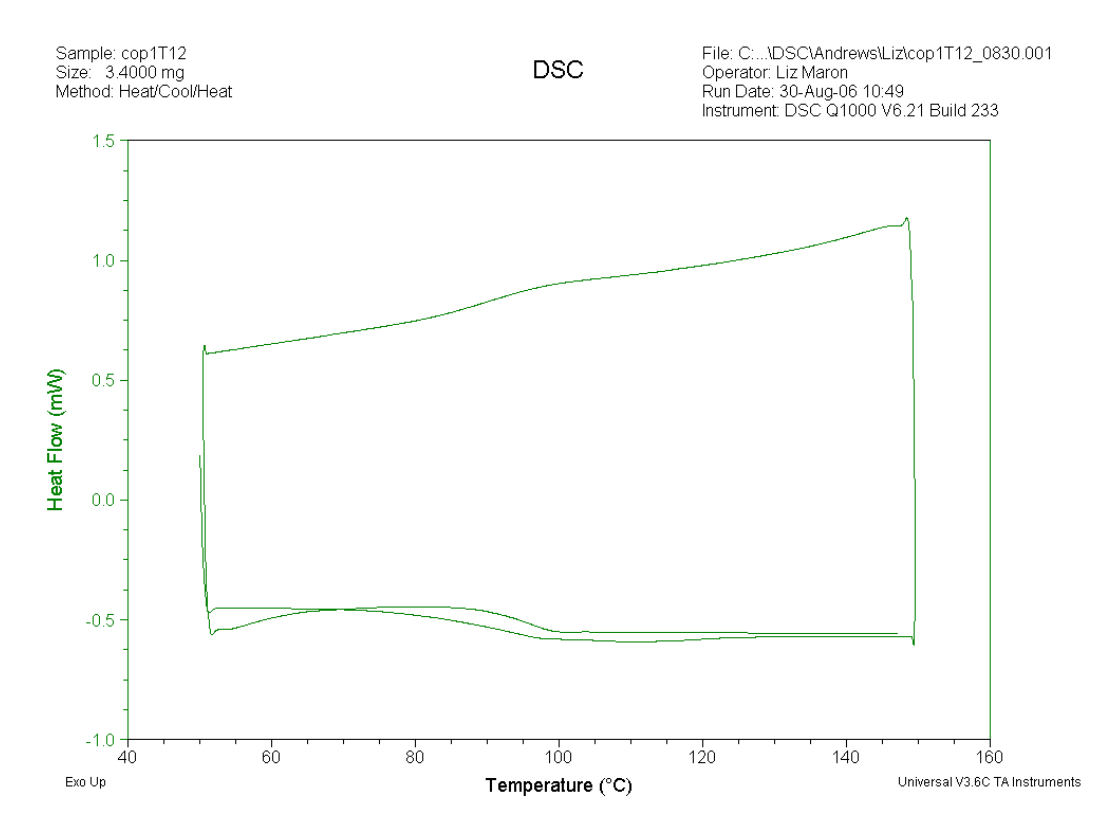


FIGURE 2.12 Differential Scanning Calorimetry Spectrum of copT12

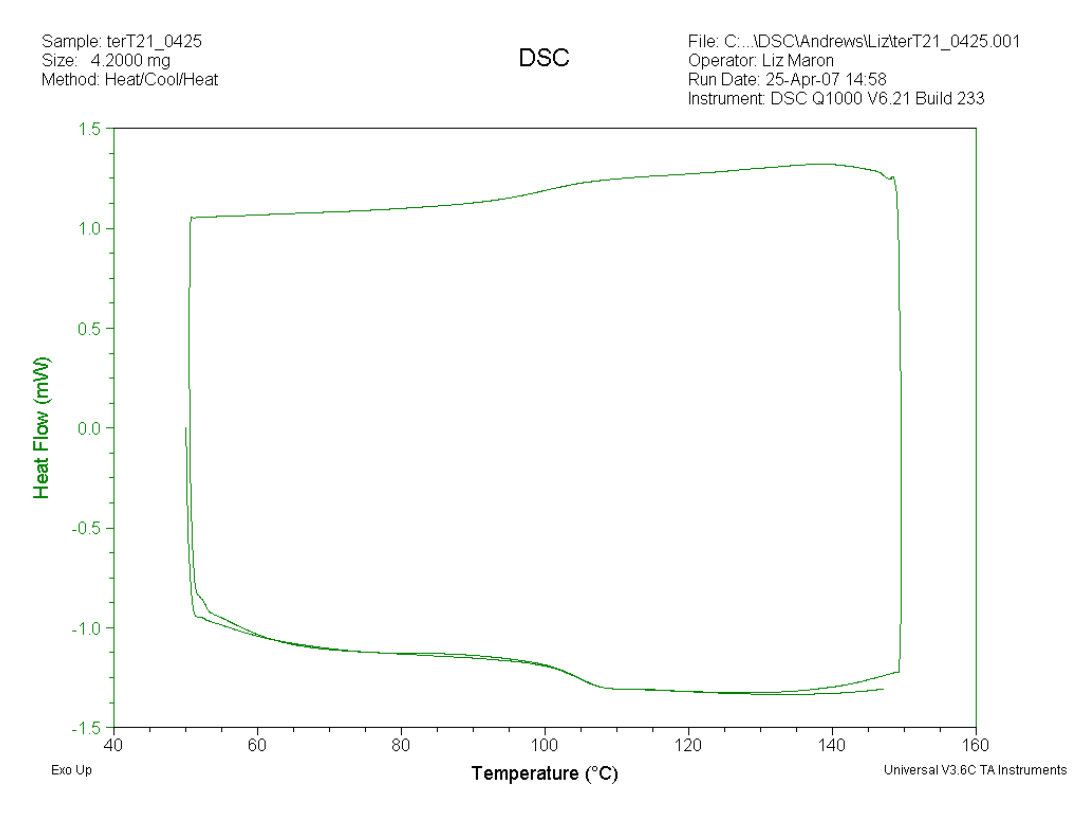


FIGURE 2.13 Differential Scanning Calorimetry Spectrum of terT21

TABLE 2.6 Summary of DSC Analysis of the Polymers

POLYMER	T _g (°C)
cop1	96.2
ter	106.0
cop2	100.3
buf	108.1

For dry pow der samples such as those analyzed here, inter- and intramolecular hydrogen bonding in the sample lessens the precision of the measurements. Static and clumping of the polymer powders results in poor contact with the sample pan, creating poor heat transfer. It is also important to note that the glass transition temperature of cured and cross-linked samples of the guiding and buffer polymers would be greater. It is difficult to observe T_g in cured polymers because motion of the chains is restricted, causing the transition step to occur over a larger temperature interval, making the temperature determination little more than an estimate.

The D SC s pectra coll ected display f ew features. There a re disc ernable glass transition slopes in both *copT12* and *tertT21*, corresponding to a single glass transition in the t ested r ange of 50-150 °C. There a re n o e ndothermic or e xothermic pe aks, indicating that the materials do not exhibit melting or crystallization in this temperature range.

2.4 CONCLUSION

Four types of styrene-based fluorinated copolymers were synthesized via radical polymerization. Characterization of this fluoropolymer family was performed by GPC, TGA, DCS, and ¹H NMR and ATR FT-IR spectroscopy. Reproducibility of these

polymers was confirmed by ¹H NMR and ATR FT-IR spectroscopy. TGA and DSC confirmed the suitability of these polymers for optical materials processing. These materials were deemed suitable for waveguide fabrication and lithography described in the following chapter.

¹ J.-P. Fouassier, *Photoinitiation, Photopolymerization and Photocuring*, Hanser Publishers: Munich, 1995.

- ⁴ C. Pitois, S. Vukimirovic, A. Hult, D. Wiesmann, M. Robertsson, *Macromolecules*, **32**, 2903-2909 (1999).
- ⁵ D.W. Van Krevelen, *Properties of Polymers: Their correlation with chemical structure; Their numerical estimation and prediction from additive group contributions*, 3rd Ed. Elsevier Science Publishers: New York, 1990. pp 138-139, p 148, p 642.
- ⁶ V.G. Gregoriou, "Fourier Transform Infrared Spectroscopy of Polymers" from *Applied Polymer Science: 21st Century*, Craver, Clara D. and Carraher, Charles E., Eds., Elsevier: Amsterdam, 2000.

- A. Peacock, Polymer Chemistry: Properties and Applications, Hanser Publishers: Munich, 2006.
- ¹¹ L.R. Dalton, A.W. Harper, B. Wu, R. Ghosn, J. Laquindanum, Z. Liang, A. Hubbel and C. Xu, *Adv. Mater.*, 7, 519-540 (1995).
- ¹² J. Brandrup, E.H. Immergut, E.A. Grulke, eds. *Polymer Handbook, 4th Edition*, John Wiley & Sons, Inc.: New York, 1999. p VI-253.
- ¹³ T. Hatakeyama and F.X. Quinn, *Thermal Analysis: Fundamentals and Applications to Polymer Science*, 2nd Ed. John Wiley & Sons, Ltd.: Chichester, England, 1999.

² S. Buscemi, A. Pace, R. Calabrese, N. Vivona and P. Metrangolo, *Tetrahedron Letters*, **57**, 5865-5871 (2001).

³ M. Fox, Optical Properties of Solids, Chapter 2, Oxford University Press: New York, 2001.

⁷ The Aldrich Library of FT-IR spectra, Edition II, Vol. 2, 1997 1743D

⁸ The Aldrich Library of FT-IR spectra, Edition II, Vol. 2, 1997 1742C

⁹ J.M. Evans, *Polymer Eng. and Sci.*, **13**, 6, 401-408 (1973).

CHAPTER 3:

WAVEGUIDE LITHOGRAPHY AND FABRICATION

3.1 INTRODUCTION

3.1.1 THE FABRICATION PROCESS

The f abrication of p olymeric opt ical w aveguide de vices involves m any complicated processing steps. Although the design of the guiding polymer as a negative photoresist in this thesis removes a number of conventional resist processing steps, fabrication is still a complex process. Process de velopment is i terative in nature, requiring careful development of each step with a focus on reprodicibility. Iterative development of each step is crucial to the creation of a robust process flow towards the desired outcome. A flow chart outlining the fabrication steps is shown below:

FIGURE 3.1 Waveguide Fabrication Flow Chart

A. SUBSTRATE

A.1 Surface Treatment

A.2 Functionalization

B. BUFFER

B.1 Surface Treatment

B.2 Spin-coat

B.3 Soft Bake

B.4 Hard Bake

C. GUIDE

C.1 Surface Treatment

C.2 Spin-coat

C.3 Pre-exposure Soft Bake

C.4 UV Exposure

C.5 Post-exposure Soft Bake

C.6 Wet Etch

C.7 Hard Bake

D. CLADDING

D.1 Surface Treatment

D.2 Spin-coat

D.3 Soft Bake

D.4 Hard Bake

The deposition of each layer requires some form of surface treatment to promote adhesion, which varies according to polymer structure and the material on to which it is applied. Spin-coating and baking conditions are unique to each polymer and are influenced by solution viscosity and composition.

3.1.2 DIRECT LITHOGRAPHIC PATTERNING

Fabrication and the direct photolithography of waveguides is depicted in the flow chart presented be low. Polymer layers are applied to the substrate in sequence. UV exposure i nitiates crosslinking in the negative resist-type guiding layer, creating waveguides tructures. The unexposed, unchanged guiding polymer is removed with acetone and the structures are buried in cladding polymer such that they are completely confined by lower-index material.

SUBSTRATE A.1-2 BUFFER B.1-4 SUBSTRATE C.5 GUIDE C.1-3 BUFFER SUBSTRATE ACETONE C.6PHOTOMASK C.7C.4 CLADDING GUIDE D.1-4 BUFFER SUBSTRATE

FIGURE 3.2 Waveguide Photolithography Flow Chart

Crosslinking occurs by the same mechanism as photopolymerization but does not include pr opagation. E very po int of c rosslinking m ay r equire t he a bsorption of a photon. Two initiators were used in different steps of waveguide preparation. For the buffer m aterial c rosslinking i s a chieved by he ating a l ayer of t he po lymer i n the presence of be nzoyl p eroxide (BPO). The gui ding m aterial is do ped w ith a photoinitator so that it may be patterned by light exposure through a lithographic mask. The e xposed por tions become c ross-linked a nd i nsoluble, f orming t he w aveguide structures, while the unexposed regions may easily be etched away by dissolution in acetone. Irgacure 184 from C iba S pecialty Chemicals is an efficient, non-yellowing initiator that a bsorbs hi ghly i n t he UV a nd was therefore selected for lithographic printing with the contact mask aligner and 350-450 nm broad spectrum UV lamp.

FIGURE 3.3 Structure of Irgacure 184, 1-hydroxy-cyclohexyl-phenyl-ketone

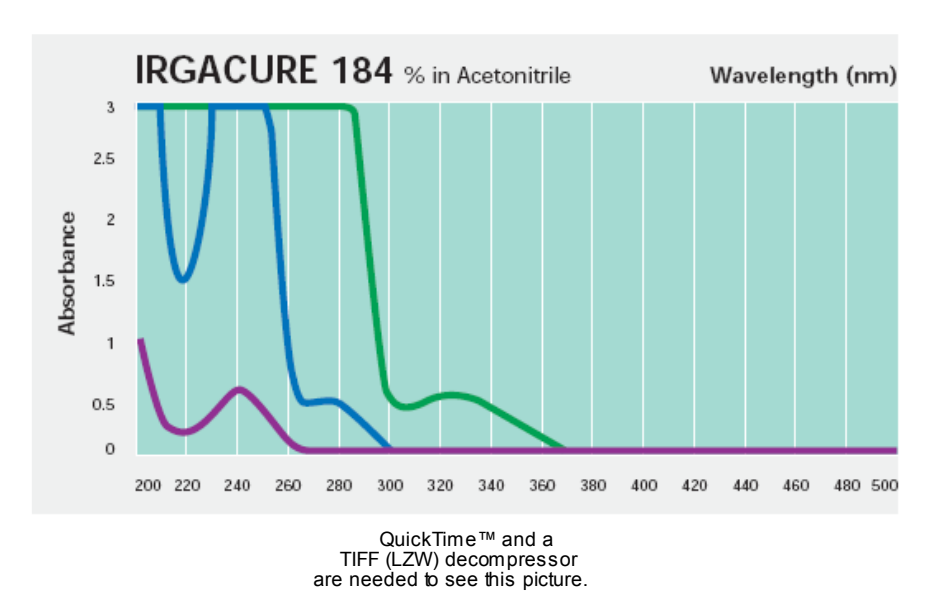


FIGURE 3.4 Absorption Spectra of Irgacure 184 in Acetonitrile at Varied Weight Percents.²

3.1.3 McGILL UNIVERSITY MICROFABRICATION FACILITY

A majority of the production of lithographically written structures was performed in the microfabrication laboratory at McGill University. This resource is part of the McGill Institute for Advanced Materials (MIAM).

The MIAM facility consists of two main cleanrooms: 1) A class 1000 certified etch and deposition cleanroom containing, among other things, plasma oxidation equipment and an optical microscope utilized in the procedures described in this chapter. 2) A class 100 phot olithography cleanroom which i ncludes t he s pin-coater, a ligner, and programmable oven used for the experiments described in this chapter. The "class" of a cleanroom indicates that its atmosphere is maintained with less than that number of particles larger than 0.5 μ m in each cubic foot of air space. This at mosphere is beneficial to the fabrication of microstructures because defects in waveguides due to dust are suppressed. The photolithography cleanroom is maintained at a temperature of 21 ± 1 °C and 47 ± 3 % relative humidity.³

3.2 EXPERIMENTAL

3.2.1 GENERAL METHODS

3.2.1.1 Sample Handling

Substrate pieces were preferably manipulated with clean, dry, Teflon or Nalgene tweezers and occasionally held by their edges with fresh neoprene gloves during their functionalization a nd t hroughout microfabrication. S olutions of materials to be spin-coated were prepared in new glass vials with screw caps or 25 mL Erlenmeyer flasks with ground glass stoppers, which were rinsed with acetone and freed of dust using compressed air.

3.2.1.2 Spin-Coating

Spin-coating was performed on a tabletop Bidtec R&D Spin-coater or Headway Research I nc. S pinner with model P WM32 c ontroller a ccording to the following programmed sequence with varied maximum spin speeds: The substrate was brought from 0 rpm to the maximum spin speed in one second, held at the maximum speed for 7 seconds, then s lowed at a deceleration of 500 rpm/s to 0 r pm. For example, if the maximum desired speed was 1000 rpm, the substrate was brought to this speed in 1 s at an acceleration of 1000 rpm/s, held at 1000 rpm for 7 s, and decelerated to 0 rpm over 2 s. This sequence was not required when using the spin-coater for rinsing or drying.

3.2.1.3 Baking

Hard baking was performed in an Isotemp Programmable Oven according to the following s equence: The temperature was ramped from 25 °C to 100 °C over 15 minutes, then raised to 200 °C over the course of an hour, held at 200 °C for two hours, and finally lowered to 25 °C over one hour. Soft baking and pre- and post-baking were performed on hot plates with clean surfaces which were pre-set to the desired temperatures.

3.2.1.4 Plasma Oxidation

Surface roughening by plasma oxidation was carried out by a Tegal 415 Oxygen Plasma Asher to prepare one polymer layer for coating by a nother. It was performed immediately prior to application of the polymer. The sequence used between 0.96 and 1.00 torr of O₂ plasma pressure and 150 W of power for 5 minutes.

3.2.2 REAGENTS AND MATERIALS

Waveguides were fabricated on 6 inch round wafers of single-side polished silicon. These wafers were 625 μ m thick and diced in the < 100 > orientation. Wafers were obtained from Nova E lectronic Materials, T exas, USA. The pol ymers us ed w ere

prepared as described in Chapter 2. Benzoyl peroxide (BPO), 97%, was obtained from Aldrich and purified according to the procedure described in Section 2.2.3.1. Irgacure 184 was obtained from Ciba Specialty Chemicals.

Sulfuric a cid (H_2SO_4) , 95.0-98.0%, and hydrochloric a cid (HCl) were obtained from ACP Chemicals and hydrogen peroxide (H_2O_2) , 30%, was obtained from Fisher. Milli-Q® water was obtained from a Milli-Q® Ultrapure Water Purification System. Isopropyl alcohol, a cetone, and tetrahyrdrofuran (THF), 99.5%, were a cquired from EMD C hemicals. T riethoxyvinylsilane (TEVS), 97%, was obtained from Aldrich. Cyclopentanone, 99+%, was also acquired from Aldrich and distilled prior to use.

3.2.3 SUBSTRATE PREPARATION

Wafers were first cleaved into appropriate dimensions, typically at least 25 x 50 mm. An identifying mark was etched into one corner of the unpolished side of each.

3.2.3.1 Piranha Cleaning

The substrate pieces were individually placed in small beakers, usually 30 or 50 mL capacity. The Piranha solution used was a mixture of 1:1 concentrated sulfuric acid added to concentrated hydrogen peroxide, prepared in a large beaker and immediately poured into the small beaker to cover each substrate completely. The substrates were left for at least 5 minutes be fore the next step was begun. One by one, they were removed from the Piranha solution and rinsed for 1-2 minutes with Milli-Q® water from a wash bot tle followed by a rinsing with i sopropanol and s pun dry on the spin-coater.

3.2.3.2 Functionalization with Triethoxyvinylsilane (TEVS)

Substrates which had been cleaned and dried according to Section 3.2.3.1 were placed polished-side up in a glass crystallizing dish which was then filled with a bath of TEVS about 1 cm high. The bath was set on a hotplate under a high flow of argon and heated to 1 30 ° C a nd m aintained a t t hat temperature f or 15 m inutes us ing a

thermocouple. The crystallizing dish was subsequently removed from heating and the argon flow maintained as it cooled. Once the temperature fell be low 30 °C, each substrate was rinsed with THF from a Pasteur pipette for 1-2 minutes followed by a rinsing with isopropanol and spun dry on the spin-coater.

The crystallizing dish was washed immediately and placed in a base bath for 24 hours or else it could never be thoroughly cleaned enough for re-use. The cleaned, functionalized substrates were placed in individual, labeled Petri dishes. Wafer pieces which were not used within one month of their functionalization were re-functionalized beginning with the piranha cleaning step.

3.2.4 APPLICATION OF BUFFER LAYER

The solution for buffer layer application consisted of 40 % wt *bufTxx* and 5 % wt BPO in cyclopentanone. Approximately 1 mL of solution was required to form a single layer on a 1x2 inch substrate. A stir bar and the full desired volume of cyclopentanone were transferred to the vial or flask used for mixing. The polymer was added in portions of 0.2-0.5 g. A new portion was not added until the previous portion had completely dissolved. For solutions containing 10 g total of *bufTxx*, this procedure often required a minimum three hours. BPO was added in the same manner, with the vial was wrapped in foil to prevent early curing, then stirred for 30 minutes before filtration.

The polymer and initiator solution was transferred to a 20 mL disposable syringe and filtered manually through 5 μ m and 1 μ m Teflon filters in sequence. This procedure was often carried out by two persons since microfiltration of the highly viscous solution required a great deal of force. The solution was allowed to stand undisturbed for 15 minutes to one hour before use to allow air bubbles to rise out of the solution that might otherwise interfere with achieving a homogenous layer.

The functionalized substrate to be coated was rinsed with isopropanol and dried on the spin-coater immediately prior to application of the polymer. 1-2 mL of polymer was then taken up in a disposable glass pipette and distributed onto the substrate surface in one slow, smooth, S-shape motion: starting in one corner and moving along the long

edge of the substrate, passing in the opposite direction through the middle, then moving along the other long edge to finish at the opposite corner. The polymer was allowed to spread for a few seconds and examined for any obvious air bubbles. If visible bubbles could not be prodded away with a pipette tip the polymer was removed by rinsing with acetone and re-rinsing and drying with isopropanol on the spin-coater before a new layer was applied. If the application was acceptable, the substrate was spun with a maximum speed of 1500 or 2000 rpm according to the program described in Section 3.2.1.2. When *bufTxx* was used as a cladding to cover the waveguide structures, it was spun to a maximum speed of 500 rpm.

After spinning, the sample was immediately transferred to a hotplate at 130 °C for 180 s f or s oft ba king. When a ll s amples i n one ba tch w ere c omplete, t hey w ere transferred to a programmable oven for hard baking according to the program described in Section 3.2.1.3. Thicker buffer layers were often desired, requiring a second coating of the *bufTxx* material. Before applying another layer, the surface of the first layer was oxidized according to the plasma treatment described in Section 3.2.1.4 for adhesion promotion. Samples were treated individually and immediately coated, spun, soft and hard baked as described above. Note that any sample which already holds a polymer layer must not be rinsed with acetone or isopropanol.

3.2.5 APPLICATION OF GUIDING LAYER AND PHOTOLITHOGRAPHY

The solution compositions required for each type of waveguide a re described below. As with the buffer material, approximately 1 mL of solution was required to form a single layer on a 1x2 inch substrate. A stir bar and the full desired volume of cyclopentanone were transferred to the vial or flask used for mixing. The polymer was added in portions of 0.2-0.5 g. A new portion was not added until the previous portion had completely dissolved. If photoinitator was required, the flask was wrapped in foil to prevent light exposure and early curing and brought to a darkroom where the photoinitiator was added under only red light and stirred for 30 m inutes be fore filtration.

The s tandard s olution for gui ding m aterial a pplication f or phot olithography consisted of 40 %wt terTxx and 5 %wt Irgacure 184 as photoinitiator in cyclopentanone. The polymer and photoinitiator solutions were filtered in the UV-free photolithography room of the McGill microfabrication facility. As with the buffer material solution, the guiding material solution was filtered manually through 5 μ m and 1 μ m Teflon filters.

If the guiding layer was to be placed directly onto a functionalized substrate, as for the size calibration of lithographic waveguide printing, the substrates were first rinsed with isopropanol before polymer application. If the guiding layer was to be applied on top of polymeric buffer material, *bufTxx*, the surface was prepared with plasma.

The pol ymer w as a pplied f rom a disposable pipette us ing t he s ame m ethod described for buffer layer application. The substrate was spun to the desired maximum spin speed. After spinning, each sample was immediately transferred to a hotplate at 60 °C for 30 s for a pre-exposure bake.

Crosslinking was initiated by I rgacure 184, a ctivated by UV exposure using an EVG 620 B ond A ligner with a 3 50-450 nm broad spectrum I amp. O ccasionally samples were submitted to flood exposure for refractive index characterization, but most often they printed using a lithographic mask to form waveguides. A representation of the mask is shown in Figure 3.5. The substrates were positioned on the aligner such that waveguides of the desired width would be printed perpendicular to the cleavage plane of the substrate. This was necessary to facilitate easy cleavage and clean edge exposure for end-coupling experiments. Samples were ideally submitted to 20 mW/cm² power density in five 12 s cycles separated by 20s of relaxation. After exposure, each sample was immediately transferred to a hotplate at 60 °C for 30 s for a post-exposure bake.

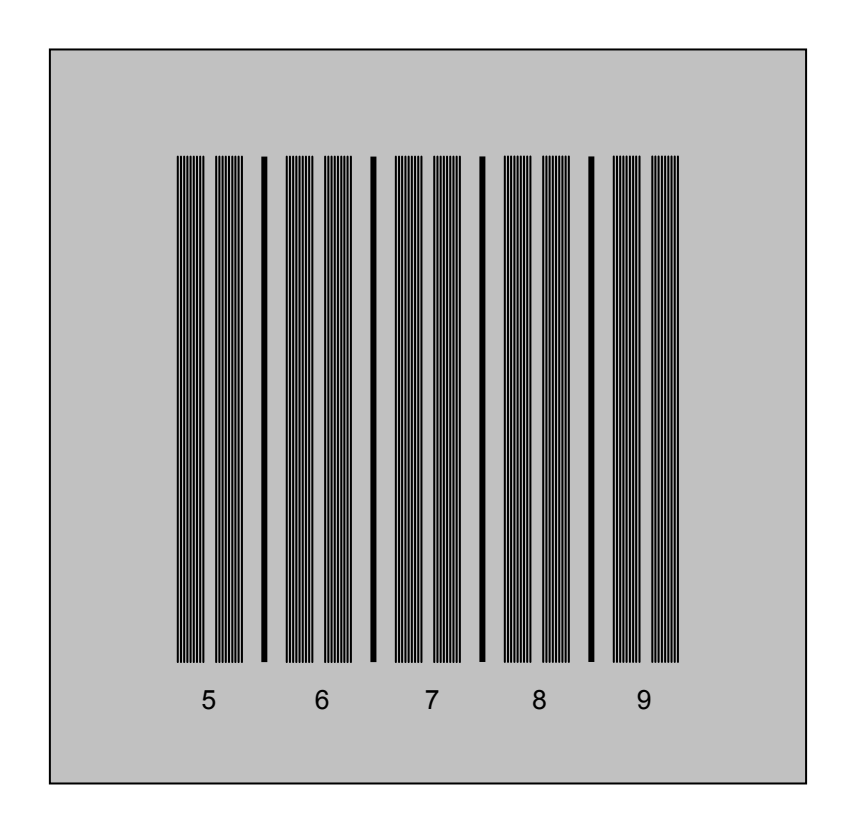


FIGURE 3.5 Representation of the lithographic mask employed to produce polymer waveguides. The mask contains five different opening widths ranging from 5 to 9 μ m. There are two groups of 9 waveguides at each width, with the different sizes labeled by printable numbers at one end of the structures and separated by a single larger opening for ease of identification.

When the lithographic mask was employed, the unexposed, uncross-linked guiding polymer was removed via etching with acetone. This was performed on each sample individually, achieved using a gentle stream of acetone from a wash bottle for 10 s, followed by a few seconds of slow swishing in an acetone bath often contained in a small (15 cm) crystallizing dish. If visible residue remained after drying the substrates were rinsed a second time. When all samples in one batch were complete, they were transferred to a programmable oven for hard baking.

3.3 RESULTS AND DISCUSSION

Many fabrication experiments were performed while working to attain the proper structure and dimensions that might be appropriate for a waveguide optical amplifier. The ideal system, a drawing of which is shown in Figure 1.2 in the introductory chapter, consists of a l ayer of buffer material greater than 10 μ m in height on which sits a straight waveguide of at least one inch in length and 6 μ m by 6 μ m in height and width. No calculations were conducted to determine the mode overlap between the optical fiber and the waveguide, so it was assumed that the 6 μ m by 6 μ m core dimensions would be an appropriate starting point for coupling a 9 μ m optical fiber. The ideal waveguide is covered by a protective cladding layer greater than 10 μ m that is either a new material with good mechanical properties for waveguide coverage or is the same composition as the buffer material. There were many variables evaluated in the effort to achieve the ideal structure and the results of this testing is presented here.

The quality of the microfabrication was evaluated with several metrology tools. Early samples were inspected via optical microscope in the microfabrication facility immediately after preparation. Although this method was limited, only top-down views of the structures could be effectively achieved, this method was useful in evaluating the amount of delamination of waveguide structures and the best procedure for structure etching. The edge-on dimensions of the printed waveguide structures (height and width) were anallyzed from strandard Scanning Electron Microscopy (SEM) and Field-emission Gun (FEG) SEM images of cross sections of cleaved samples. It was determined early on that the softness of the polymer material made it a better candidate for FEG SEM in order to obtain clear images for quantitative analysis. Standard SEM images exhibited artifacts from surface charging, as seen in Figure 3.9b. A Metricon prism coupler was sometimes employed to determine layer thickness and more commonly used to determine the refractive in dex of the polymer materials, a very important variable in waveguide fabrication.

3.3.1 SUBSTRATE FUNCTIONALIZATION

First, to promote polymer adhesion to the silicon surface, the substrates were functionalized with T EVS as detailed in 3.2.3.2. It was found that without this functionalization, both *bufTxx* and *terTxx* would form inhomogeneous layers which delaminated easily from the substrate. Freshly coated TEVS substrates were used to achieve optimal adhesion. The functionalization was confirmed by a wetting test. TEVS layers exhibit hydrophobicity, forming distinct water droplets on their surface.

3.3.2 APPLICATION OF BUFFER LAYER

Initial applications of the buffer layer were carried out with only one polymer coating. It was soon determined via Metricon prism coupler and FEG SEM analysis that multiple layers were necessary to achieve the desired buffer thickness. Thick layers are required to prevent the evanescent field of the core-guided wave from coupling to the Si wafer. The latter has a complex refractive index at optical frequencies, and insufficient buffering will allow power to be lost to the substrate.

Polymer coatings were derived from solutions that contained 40 %wt of *bufTxx* in cyclopentanone (plus 5 %wt BPO). Higher concentrations resulted in inhomogeneities in the solution and problems in microfiltration. It was also determined that the polymer could not be spun with a maximum speed be low 1500 r pm without causing visible surface de fects. It is particularly important that the buffer layer, as a base for the waveguides, be smooth. The average thickness of a single layer of 40% wt *bufTxx* at a maximum spin speed of 1500 rpm was 6 μm.

Some samples were prepared with two layers of buffer material to improve decoupling of the core from the substrate. The initial layer was applied to a TEVS functionalized surface while the second was applied immediately after plasma oxidation of the first layer. The average thickness of two layers of bufTxx each spun to 1500 rpm was 11 μ m. Plasma oxidation removed some material, reducing the total height.

3.3.3 APPLICATION OF GUIDING LAYER

Early experiments involving lithography of the guiding material were carried out directly on the substrate surface in order to conserve buffer material. Many variables come in to play in waveguide fabrication and a certain degree of control over these was desired before attempting more resource-consuming experiments.

3.3.3.1 Calibration of Layer Thickness

First a calibration curve of the variation in guiding layer thickness to spin speed was completed. This was much more important for the guiding layer, where we were working t oward a c ertain s tructure di mension, t han f or t he buf fer l ayer. Guiding polymer was applied directly to TEVS functionalized substrates, spun to maximum speeds between 1250 and 2500 rpm in 250 rpm increments and cured with the standard UV flood exposure program described in Section 3.2.5.1. They were then rinsed with acetone from a disposable pipette for 20 s econds to replicate etching conditions and hard baked. Two additional samples prepared at 1500 and 2500 rpm were left un-etched. The summarized results in Figure 3.6 are the average of three measurements of each sample.

The samples exhibited an inverse relationship between maximum spin speed and layer thickness. The sample spun to 1250 rpm exhibited surface defects, indicating in general that low spin speeds are inappropriate for obtaining homogeneous polymer layers. The un-etched samples exhibited a greater than expected thickness difference from their etched counterparts. It was later discovered that guiding layers placed on buffer polymer experience less degradation from a cetoner insing owing to less scattering loss and more complete curing. Figure 3.7 shows two waveguides prepared with identical guiding polymer processing conditions. The structure formed on a buffer layer is thicker than the structure placed directly on the substrate. The top surfaces of these waveguides exhibit rounded corners due to etching. This feature is less pronounced in the structure on a buffer layer because it is more densely crosslinked.

The small outward curves at the bases of the structures are formed by backscattering at the lower surface of the guiding polymer.

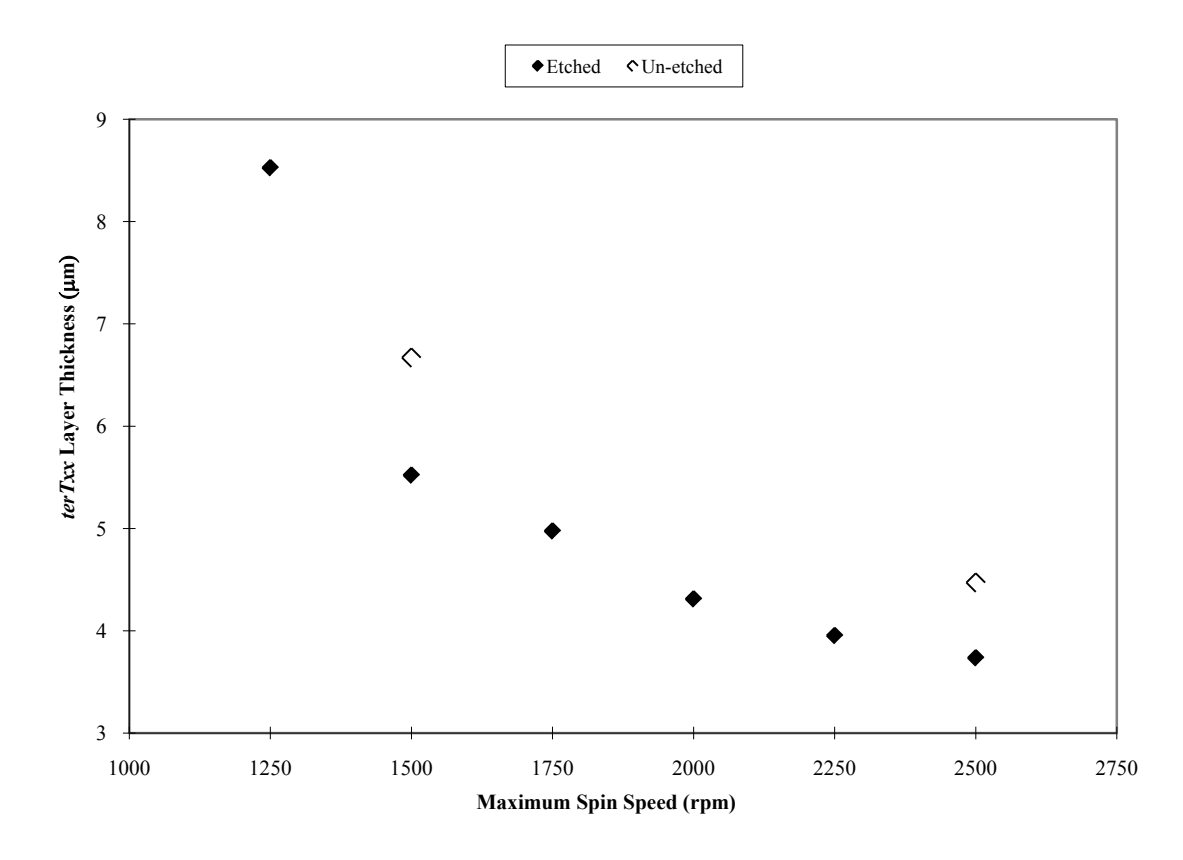


FIGURE 3.6 Calibration of *terTxx* polymer layer thickness for the spin-coating program in Section 3.2.1.2. "Etched" samples were rinsed with acetone prior to hard baking.

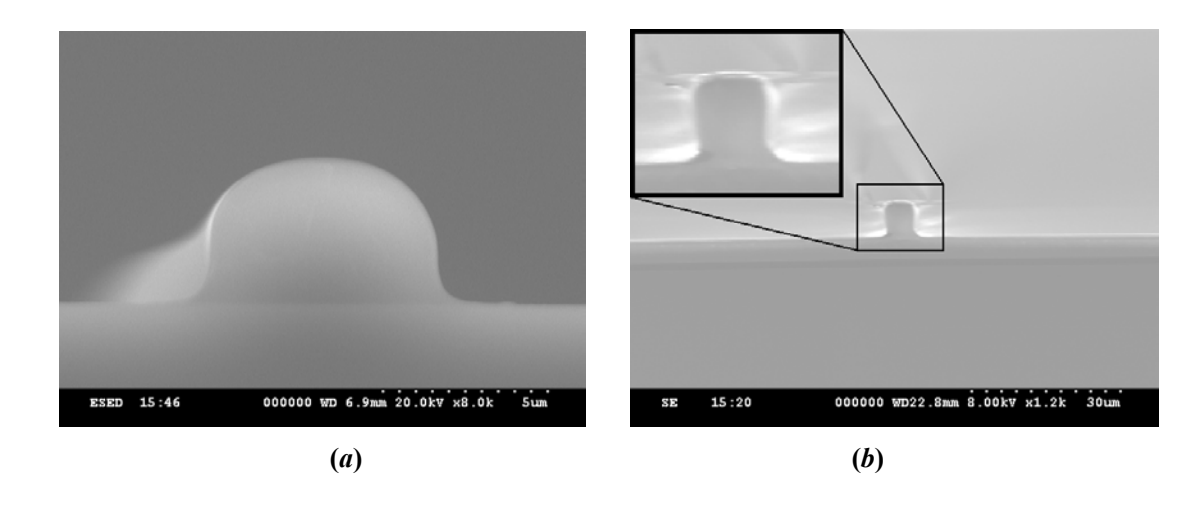


FIGURE 3.7 FEG SEM images of waveguide structures prepared at maximum spin speed of 2000 rpm with 60 s UV exposure at 20 mW/cm² printed from a 7 μ m mask opening and (a) applied directly on a functionalized silicon substrate and (b) applied on a buffer layer.

3.3.3.2 Optimization of UV Exposure

The effect of U V exp osure on f eature he ight w as exa mined by curing films deposited at two different spin speeds with three different exposure programs at a power density of 20 m W/cm². The standard program consisted of five 12 s flood exposures separated by 20 s intervals for 60 s total exposure time. The "double" program had 120 s exposure time over ten cycles and the "quadruple" had 240 s exposure time over twenty cycles. Following exposure, the substrates were rinsed with acetone to mimic feature processing conditions. The results are summarized in Figure 3.8.

It was determined that waveguide thickness increased with exposure time for the same power density by a similar trend for films deposited at 1750 and 2000 rpm. Longer UV exposure promotes additional polymer crosslinking, reducing the effect of scattering loss in the Si substate. The guiding layer is hence less susceptible to removal with etching. The films exposed for 120 and 240 s exhibited thicknesses close to extrapolated values for un-etched layers from Figure 3.6, indicating little degradation by acetone. This increasing trend is less significant from double to quadruple exposure owing to the limit of available crosslinking moieties.

The variation in waveguide structure widths with UV exposure time was examined next to determine if longer exposures were appropriate. Waveguides produced in the initial tests were printed without buffer layers, with 60 s of UV exposure. These structures were found to be 0.5-1.0 μ m wider than the lithographic mask opening used. Waveguides which were printed on top of buffer material under the same conditions gave structures \pm 0.2 μ m the width of the mask opening used. Higher exposure times produced m uch w ider s tructures with i rregular, hi ghly s loped s ide walls due to increased c rosslinking a nd some backscattering. Figure 3. 10 is a nexample of this undesirable shape. It was determined that only the 60 s, standard exposure program should be used. The results for 60 and 240 s exposures are presented in Figure 3.9.

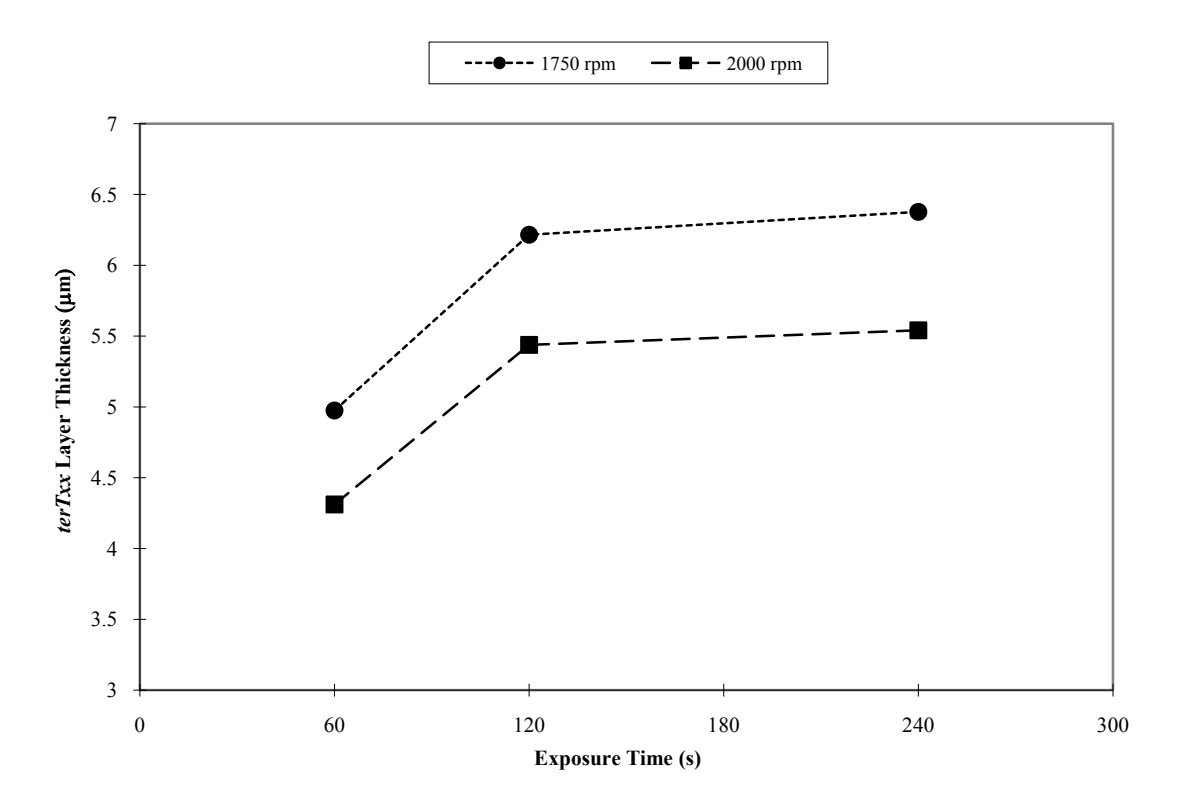


FIGURE 3.8 Calibration of *terTxx* Polymer Layer Thickness at Different UV Exposure Times and Spin Speeds

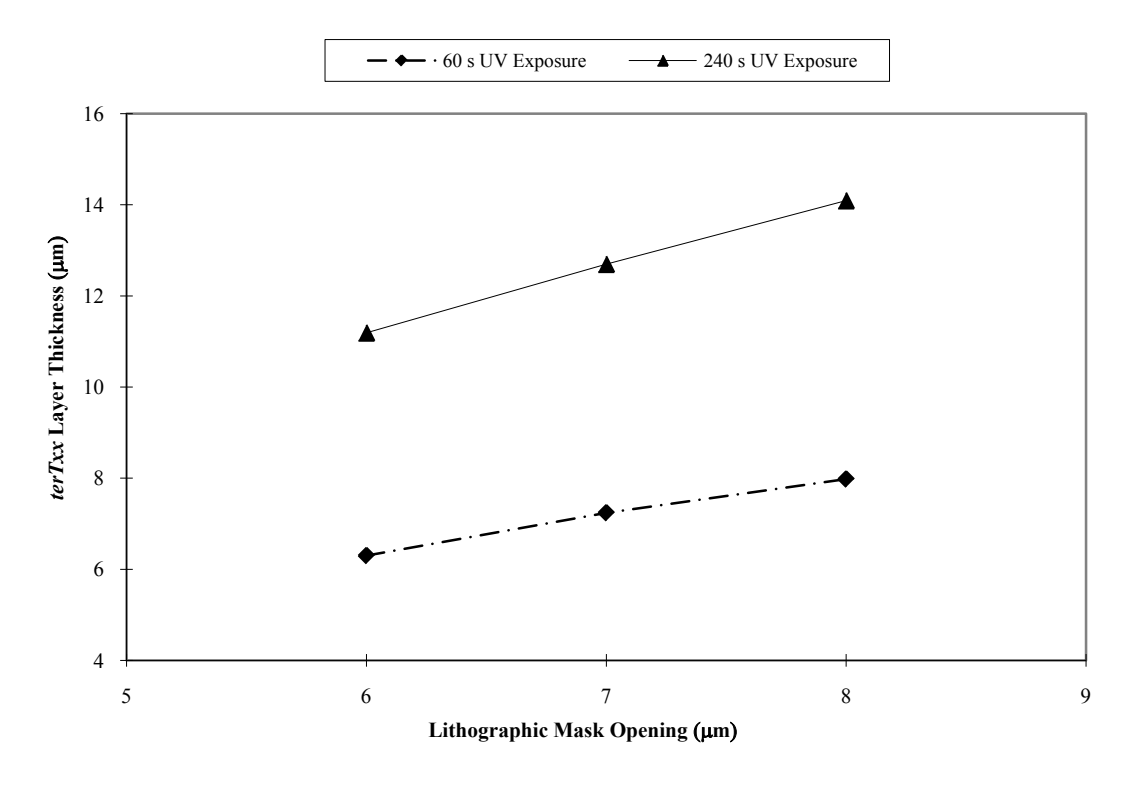


FIGURE 3.9 Calibration of terTxx Polymer Structure Width at Different UV Exposure Times

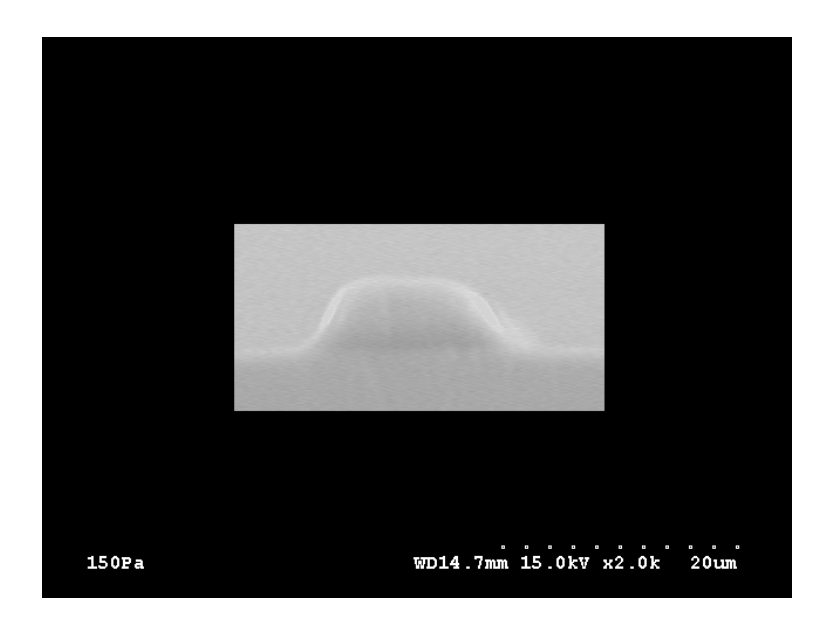


FIGURE 3.10 FEG SEM image of a waveguide structure prepared at maximum spin speed of 2000 rpm with 240 s UV exposure at 20 mW/cm² printed from a 7 μm mask opening on a buffer layer.

3.3.3.3 Optimization of Etching Conditions

An evaluation of the etching conditions was performed to find a method which would be effective in removing uncross-linked polymer but gentle enough to preserve the lithographic structures. Samples of *terTxx* were prepared under standard conditions and spun to a maximum speed of 2500 rpm. A summary of the etching analysis in presented in Table 3.1.

TABLE 3.1 Comparison of acetone etching methods used to remove uncross-linked guiding polymer and reveal printed waveguide structures. Complete samples were examined by standard optical microscopy and cross-sections were examined by FEG SEM.

	METHOD				RESULTS		
SAMPLE	Acetone Delivery	Time	# of Repetitions	Dry Between Reps?	Degree of Deterioration	% of Cross-sections with Residue	% of Clean Cross-sections
1	dipping	10 s	10	no	moderate	>50%	20%
2	swishing	10 s	2	yes	low	10%	90%
3	swishing	20 s	1	yes	moderate	5%	95%
4	swishing	30 s	2	yes	high	5%	95%
5	rinsing	10 s	1	N/A	low	~50%	~50%
6	rinsing	30 s	1	N/A	high	N/A	N/A

The first type of etching used simple dipping in which the sample was submerged for ten repetitions of 10 s into a fresh bath of acetone with the waveguide structures oriented perpendicular to the liquid surface. FEG SEM images of the waveguides on this sample revealed significant deterioration of some of the structures, likely owing to the long time t hey were w et w ith acet one. A r epresentative sample of one such waveguide is presented in Figure 3.11a.

Overexposure to acetone swells the polymer structures making them "softer," causing them to wrinkle or collapse into irregular shapes as solvent is removed during hard baking. A majority of the structures on Sample 1 exhibited smooth, regular sidewalls but only 20 % of the examined waveguide cross-sections were completely cleaned of residual polymer. Both images in Figure 3.9 have visible residue on their right sides.

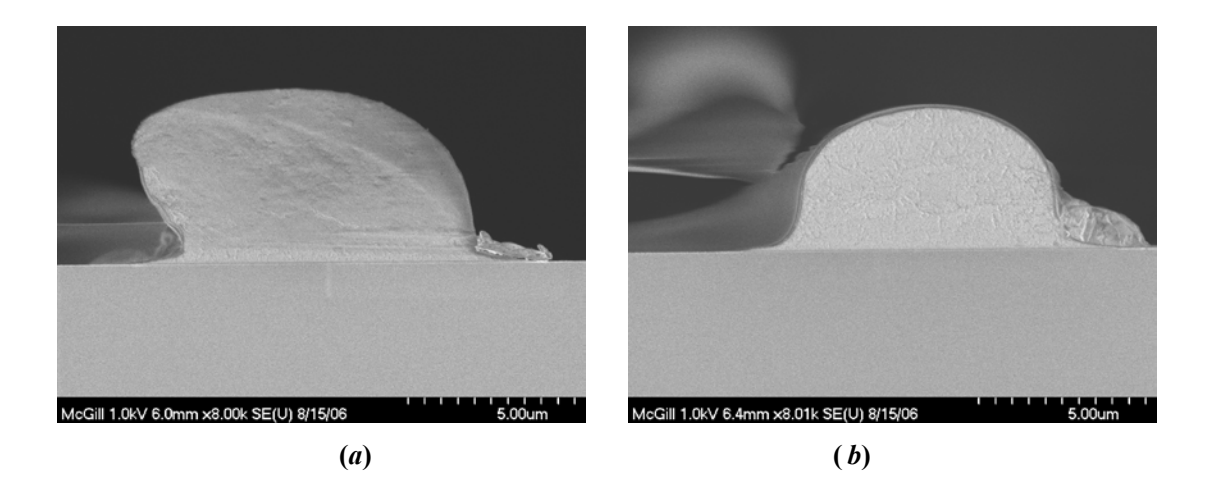


FIGURE 3.11 Standard SEM images of waveguides from etching test Sample 1: (a) Deteriorated structure printed from an 8 μ m mask opening and (b) Significant polymer residue on the right side of a structure printed from a 7μ m mask opening.

The second type of etching involved submersion and slow manual agitation in an acetone bath. This method was most successful in removing residue but resulted in deformation of the structures at longer soak times. Figure 3.12 shows SEM images of

structures from Samples 2-4, which were agitated by hand. All exhibit a higher degree of r ounding t han s amples etched by dipping or r insing and some waveguides on Samples 3 and 4, s uch a s F igures 3.12b and 3.12c, showed asymmetrical leaning. Furthermore, the optical microscope images of Sample 4 in Figure 3.13 show very little residual polymer but reveal snaking of the smaller-width structures. These structural flaws were the result of overexposure to acetone and polymer swelling.

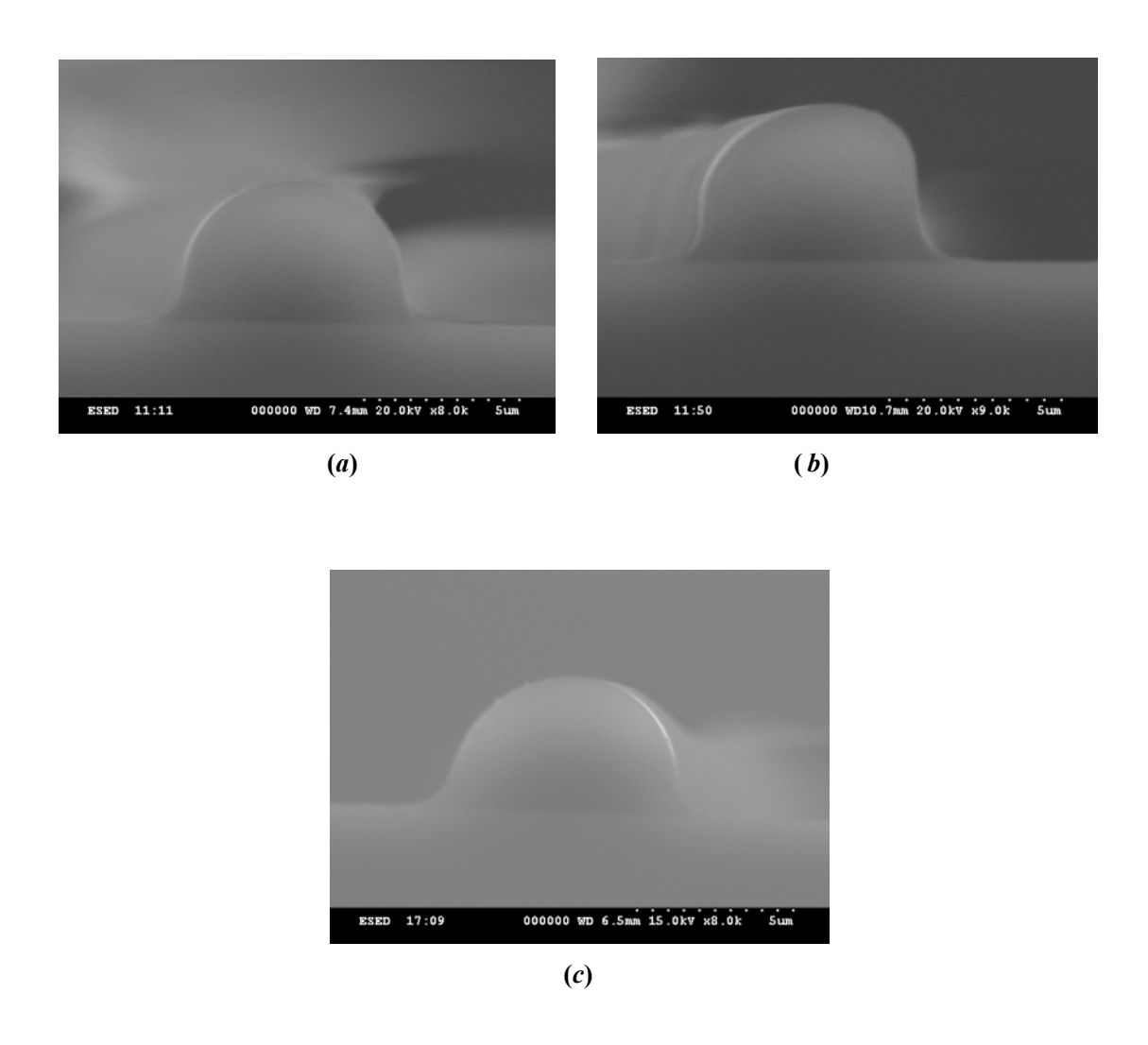


FIGURE 3.12 FEG SEM images of waveguides printed from a 6 μm mask opening from (a) etching test Sample 2, (b) Sample 3, and (c) Sample 4.

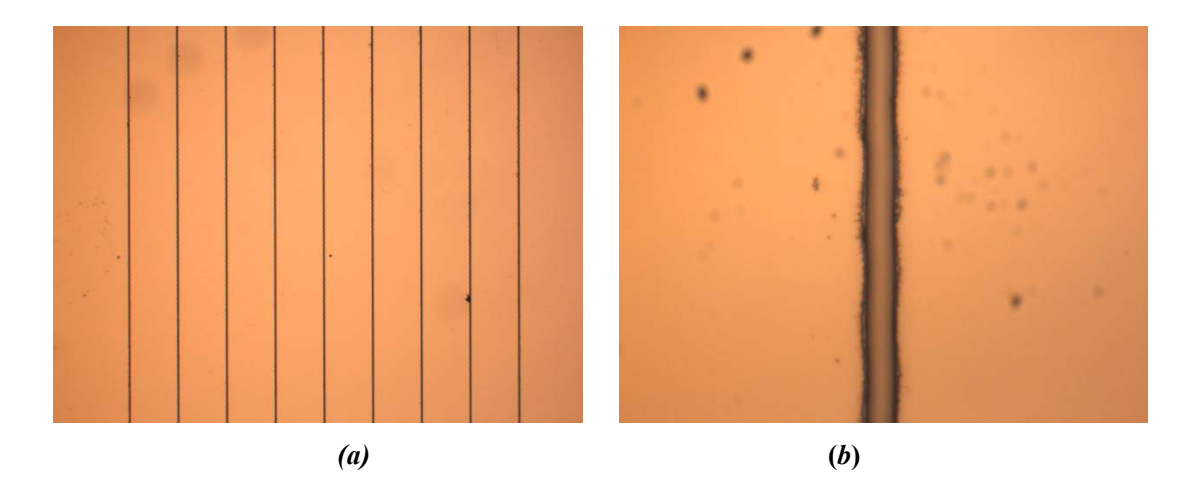


FIGURE 3.13 Optical microscope images of Sample 4: (a) 5x magnification of waveguides printed from $5 \mu m$ mask openings and (b) 100x magnification of snaking in a waveguide printed from a $6 \mu m$ mask opening.

The final type of etching was continual rinsing with a cetone from a disposable pipette. This was performed with the substrate positioned so that the flow of acetone would run down the waveguides. For Sample 5, which was rinsed for 10 s, about half of the waveguide cross-sections were clean as in Figure 3.14b and half showed a great deal of residue and irregularity as in Figure 3.14a.

The walls of clean structure cross-sections were straighter than those samples etched in an acetone bath. Optical microscopy showed no snaking effect but none of the structures were sufficiently clean for waveguiding. The polymer residue appearing between structures in Figure 3.15a seems to have been lifted from the substrate surface but never washed away.

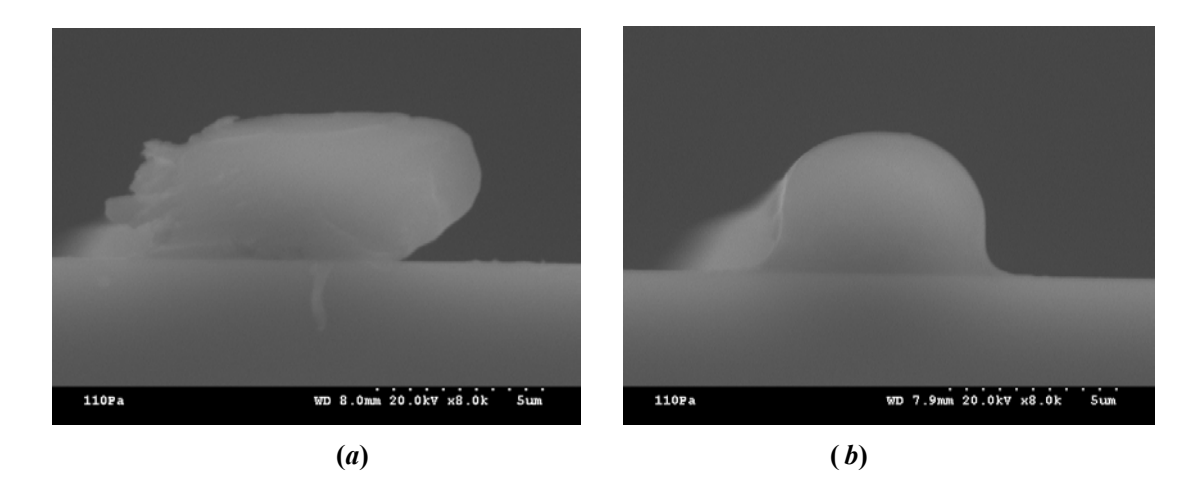


FIGURE 3.14 FEG SEM images of waveguides printed from a 6 μ m mask opening from etching test Sample 5: (a) Cross-section with irregular shape and polymer residue and (b) a clean cross-section.

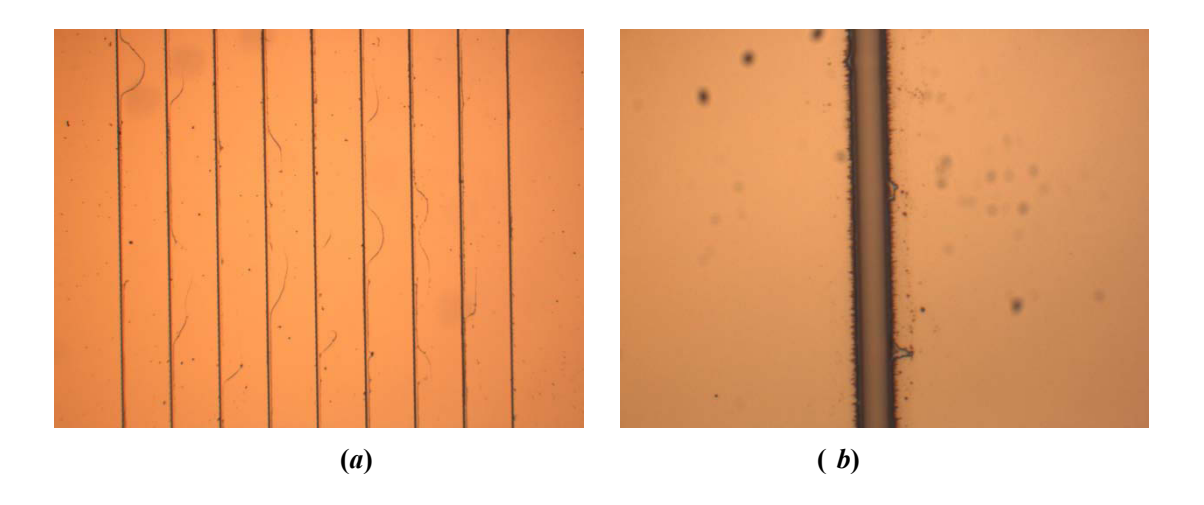


FIGURE 3.15 Optical microscope images of Sample 5: (a) 5x magnification of waveguides printed from 6 μ m mask openings and (b) 100x magnification of residue on a waveguide printed from a 6 μ m mask opening.

Sample 6, which was rinsed for 30 s, showed a high degree of delamination and was deemed unacceptable for waveguiding by simple visual inspection.

The etching method established from these results consists of two rounds of 10 s rinsing with acetone from a pipette followed by a few seconds swishing in an acetone bath to remove polymer residue. The sample is allowed to dry between rinses to prevent over-saturation with acetone and deterioration.

3.3.3.4 Refractive Index Analysis

Prism coupling analysis was used to obtain the refractive index of the waveguide core material using a Metricon model 2010M with a wide index prism operating at 1.31 μ m. The tested samples were uncovered, unpatterned layers of guiding polymer to accommodate the Metricon prism. Results were collected from some samples with had been r insed with acetone and some which had not. The value of n for individual samples was the average of two or three measurements.

A test of unrinsed samples from a single processing batch yielded $n = 1.5212 \pm 0.0002$. Unrinsed samples from a different batch with the same processing conditions yielded $n = 1.5218 \pm 0.0002$. This small disparity indicates that the structures can be fabricated with r eproducible optical properties. A cetone-washed guiding polymer layers from the second processing batch yielded $n = 1.5206 \pm 0.0002$. This slightly lowered index can be attributed to the acetone rinsing. As discussed elsewhere in this thesis, acetone uptake causes the polymer to swell and may create air voids in the material or surface irregularities, which lowers n as a result.

3.3.4 APPLICATION OF BUFFER LAYER AS CLADDING

To complete the waveguide device, the buffer polymer, *bufTxx*, was applied as a cladding layer. It is difficult to observe distinct layers of our materials by electron microscopy due to the structural similarity of the polymers. Figure 3.16 below is the cross-section of a complete waveguide device: guiding polymer cores approximately 7 µm in diameter lithographically written on a 11 µm buffer layer and covered with a 24 µm layer of cladding. The waveguide cores are indistinguishable from the bulk polymer and there is only a small observable contrast where the buffer and cladding layers meet.

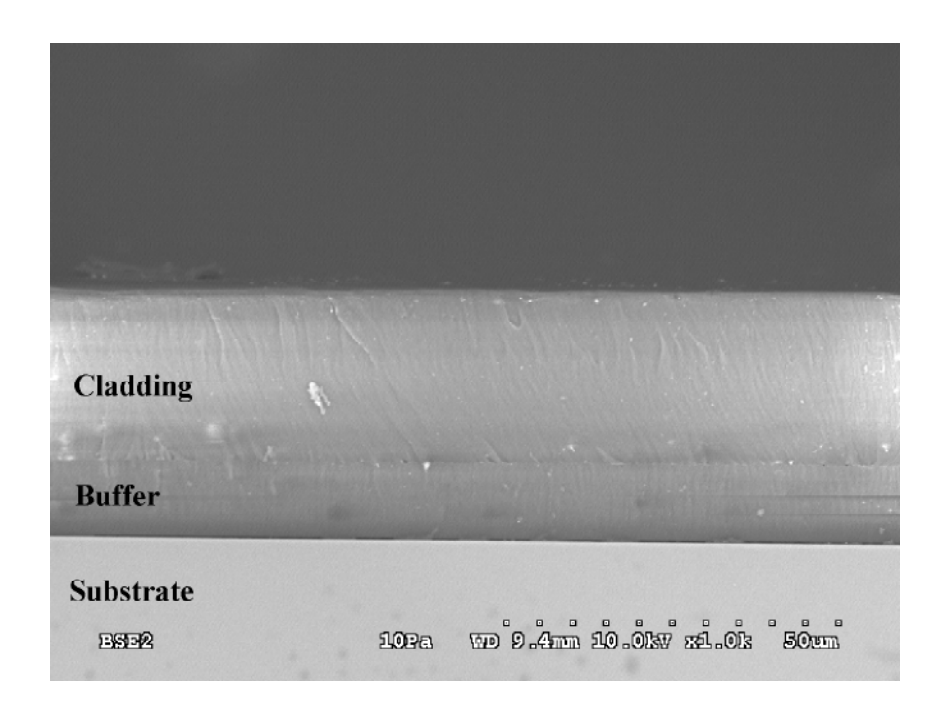


FIGURE 3.16 FEG SEM image of a complete buried waveguide device cross-section. The device sits on a silicon substrate and consists of a *bufT04* buffer layer, *terT21* guide structures (*not visible*), and a *bufT05* cladding layer.

3.3.5 END-COUPLING IN LITHOGRAPHIC STRUCTURES

Light propagation was observed in multiple printed polymer waveguide structures on multiple samples by end-coupling. End-coupling, briefly di scussed i n Section 1.1.2, was achieved using the set up pictured in Figure 3.17. This configuration is used to e valuate optical loss in fabricated waveguides. It has the advantage that it can evaluate arrays of waveguides on a single Si substrate chip by simple translation.

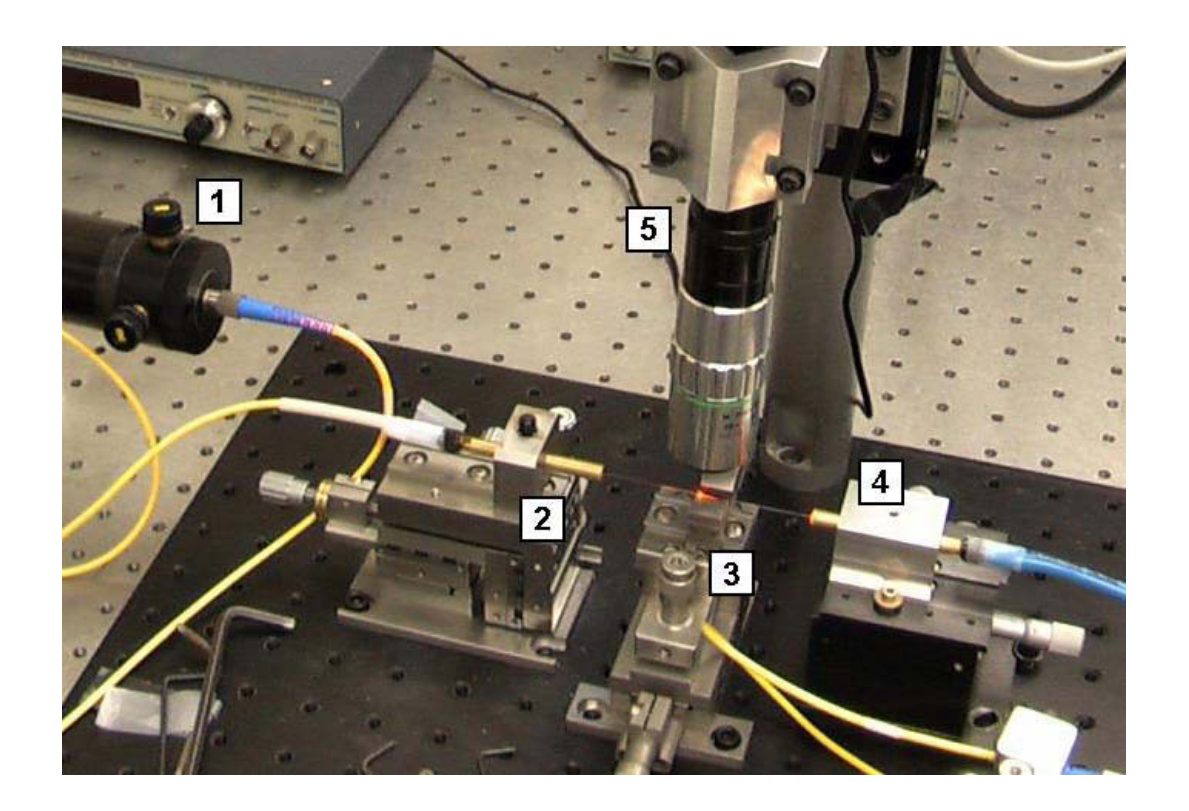


FIGURE 3.17 End-Coupling Set up

- 1) 632 nm HeNe laser
- 2) Input fiber, connected to 1. The last two inches have been stripped of bulk cladding, revealing a 9 μ m diameter fiber core surrounded by a silica buffer 125 μ m in diameter. This is supported on a translation stage to facilitate coupling to waveguide structures.
- 3) Sample holder, mounted on a translation stage.
- **4)** Collection fiber, same as **2**. To be coupled to the back end of the waveguide structures, supported on a translation stage and connected to a detector.
- **5)** Microscope and camera, connected to an external video monitor (*not shown*) for improved control during coupling.

Wafers to be exa mined were cleaved perpendicular to the waveguide direction to remove the edge bead resulting from spin-coating and produce a clean coupling surface. Cleaving also created s harp, clean facets for injecting light from the end-coupled optical fiber. Two pieces approximately 1.5 cm square were made from each sample.

A waveguide mode was observed in waveguide structures of dimensions $6 \mu m \times 6 \mu m \times 1.5 cm$ on $6 \mu m$ buffer material and $7 \mu m \times 6.5 \mu m \times 1.5 cm$ on $11 \mu m$ buffer material. Because the fiber core was larger than the complete waveguide, it was easier to couple into structures which were not covered with a layer of buffer or cladding.

However, these unprotected structures do not confine the optical power with only an air cladding so material characteristics such as loss were not measured.

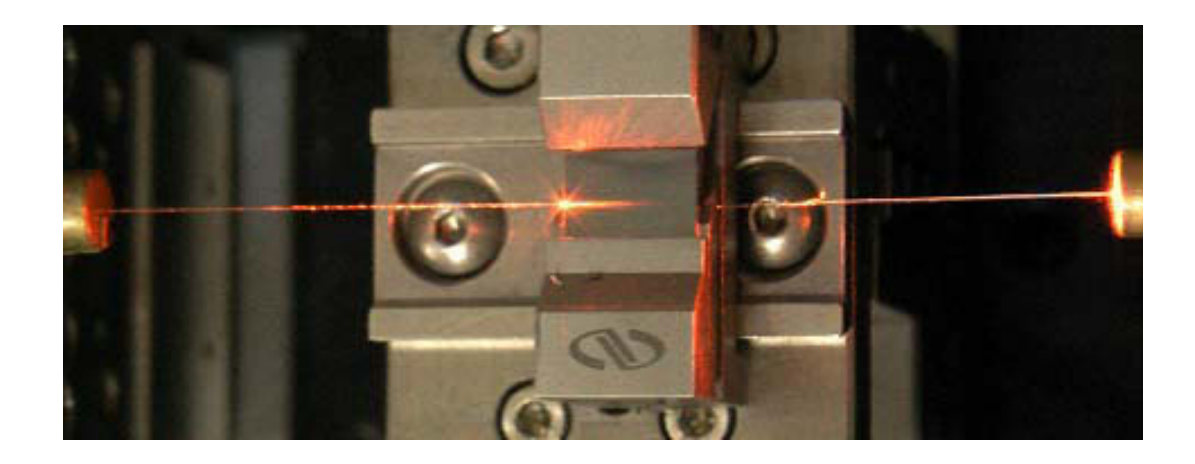


FIGURE 3.18 Light from a 632 nm source laser enters a 7 μ m x 6.5 μ m x 1.5 cm polymer waveguide structure from an input fiber (on the left) and passes through to enter the collection fiber aligned to receive light as it exits the waveguide.

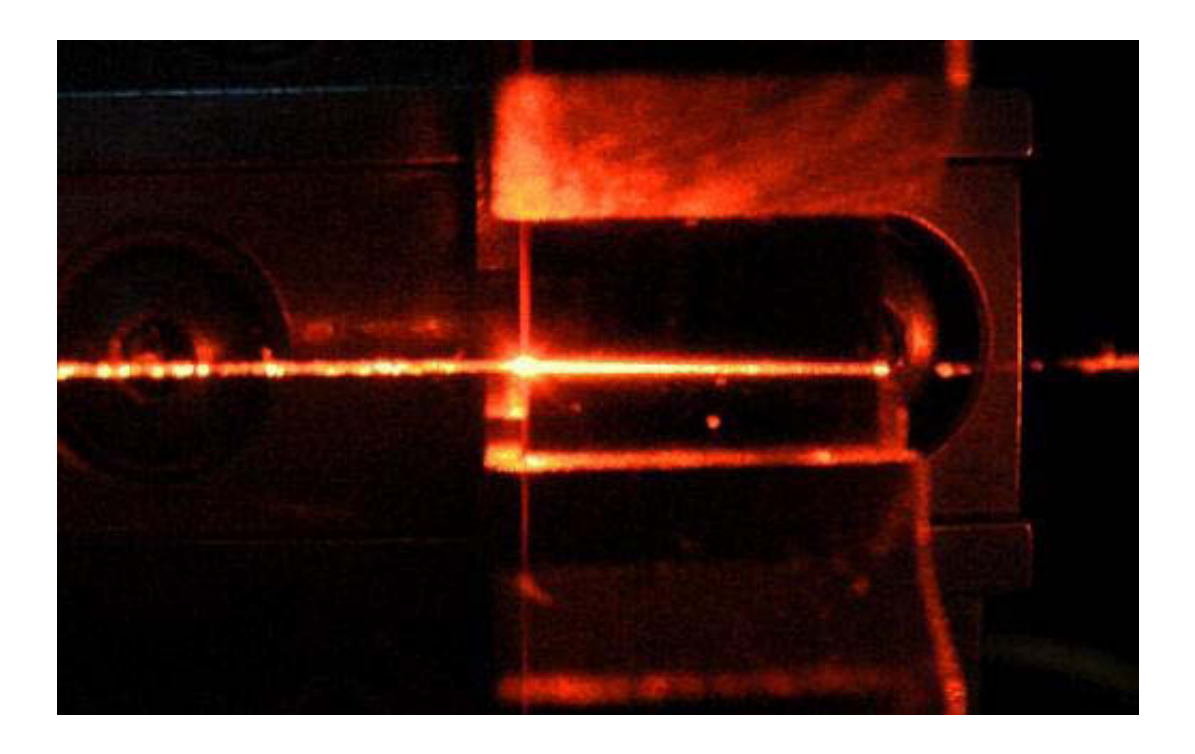


FIGURE 3.18 The waveguide from Figure 3.15 in darkness for improved contrast.

3.4 CONCLUSION

Waveguide f abrication proc esses w ere de veloped for ne gative resist-type photosensitive fluoropolymers. These materials and waveguides were characterized by optical m icroscopy, p rism c oupling analysis, and FEG SEM. Photolithographic techniques were developed to produce guiding structures with a reproducible refractive index under a variety of processing c onditions. Waveguide ar chitecture and core dimensions can be controlled to achieve appropriate devices for end-coupling with an optical fiber.

SUMMARY

This t hesis has presented the successful design and reproducible synthesis of fluorinated copolymers for use in optical waveguides. A negative resist-type guiding polymer was developed. Fabrication processes were established for each layer of a buried waveguide device. The guiding polymer was demonstrated to be reproducibly patterned into rib waveguide structures by photoinitiated lithography. The waveguides exhibited a high refractive index and successfully couple light from an optical fiber. These m ethods can be ada pted to evaluate o ther optical characteristics of the waveguides and improve optical output.

¹ J.-P. Fouassier, *Photoinitiation, Photopolymerization and Photocuring*, Hanser Publishers: Munich, 1995.

² Photoinitiators for UV Curing: Key Products Selection Guide, Ciba Specialty Chemicals, Inc.: Switzerland, (2003).

³McGill Institute for Advanced Materials website: http://miam.physics.mcgill.ca/miam/microfab/cleanroom.aspx